Partículas de prueba con espín en experimentos tipo Michelson y Morley

A Dissertation
Presented to the Faculty of Science
of
Universidad Nacional de Colombia
in Candidacy for the Degree of
Doctor of Philosophy

by
Nelson Velandia-Heredia, S.J.

Dissertation Director: Juan Manuel Tejeiro, Dr. Rer. Nat.

November 2017

Abstract

Partículas de prueba con espín en experimentos tipo Michelson y Morley

Nelson Velandia-Heredia, S.J.

2018

Resumen

En esta tesis, nosotros caracterizamos, con ayuda de la relatividad numérica, los efectos gravitomagnéticos para partículas de prueba con espín cuando se mueven en un campo rotante. Dado este propósito, nosotros resolveremos numéricamente las ecuaciones de Mathisson-Papapetrou- Dixon en una métrica de Kerr. Además, estudiaremos la influencia del valor y la orientación de espín en el efecto reloj.

Palabras clave: Relatividad general, relatividad numérica, ecuaciones de Mathisson-Papapetrou-Dixon, métrica de Kerr, partículas de prueba con espín.

Abstract

In this thesis, we characterize, with help of the numerical relativity, the gravitomagnetic effects for spinning test particles when are moving in a rotating field. Since this aim, we numerically solve the Mathisson-Papapetrou-Dixon equations in a Kerr

metric. Also, we study the influence of value and orientation of the spin in the clock effect.

Keywords: General relativity, numerical relativity, Mathisson-Papapetrou-Dixon equations, Kerr metric, the spinning test particles

Contents

List of Figures

Chapter 1

Introduction

Historically one of the problems that the General Theory of Relativity has studied is the description of the movement of a mass distribution in a gravitational field. The importance of this topic is heightened when dealing with astrophysical phenomena such as accretion discs in rotating black holes [1], gravitomagnetics effects [2] or gravitational waves induced by spinning particles orbiting a rotating black hole [3]. Our approach for this mass distribution, which has small dimensions compared with the central massive body [4], is to study the set of equations of motion for a spinning particle in a rotating gravitational field. Thereafter, we calculate numerically the trajectory for a spinning test particle when it is orbiting around a rotating massive body. The aim of this thesis is to give a numerical solution to the full set of equations for a spinning test particle orbiting around a rotating field.

To study the problem of motion of spinning test particles in an axially symmetric metric, we will use two different formulations that had been worked: The formulation of the Mathisson - Papapetrou - Dixon equatios (MPD equations) [5] and the Carter´s equations [6]. The MPD equations describe the motion of a spinning body which is moving in a rotating gravitational field. This set of equations is deduced by the

multipole expansion of the energy-momentum tensor of a distribution of mass in the middle of a gravitational field with a density of angular momentum (a). For the momenta, of lower order, the equations relate the linear and angular momentum of an extended body around a central mass with rotation. For the Carter´s equations, the equations are deduced by the first integrals of motion which relate the constants of motion such as the energy (E), the angular momentum (J), and the mass (M). Carter uses another constant of motion (Q) which relates the angular momentum of test body with the latitudinal motion of a body around a rotating mass.

With regard to the MPD equations, these equations study the problem of motion in a distribution of mass in a rotating gravitational field and were researched initially by Papapetrou [7] and Mathisson [8]. They, to study this motion, calculated a multipole expansion of symmetric momentum - energy tensor ($T^{\alpha\beta}$) which represents the distribution of mass in a rotating gravitational field [9] and from this expansion, they yielded a set of equations which includes both the monopole and dipole momentum for studying the motion of a spinning test body in a gravitational field [8]. Then, Dixon took up this system of equations [10], and defined the total momentum vector and the spin tensor for an extended body in an arbitrary gravitational field. In a paper, Dixon studied the particular case of extended body in a Sitter universe and used the spin supplementary condition $u_\beta S^{\alpha\beta} = 0$ to define the center of mass [10].

The majority of works that one finds are centered on the description of orbits around a rotating massive bodies in the equatorial plane. Tanaka *et al.* [1] using the Teukolsky formalism for the perturbations around a Kerr black hole calculate the energy flux of gravitational waves induced by a spinning test particle moving in orbits near the equatorial plane of the rotating central mass [3]. They use the equations of motion for a spinning particle derived by Papapetrou, introduce the tetrad frame and evaluate the equations of motion in the linear order of the spin with the aim of

calculating the waveform and the energy flux of gravitational waves by a spinning particle orbiting a rotating black hole. In the analytical solution given by Tanaka *et al.,* the spin value is fixed and orthogonal to the equatorial plane ($S_\perp$). Another work that uses an approximation method for describing the influence of spin on the motion of extended spinning test particles in a rotating gravitational field is made by Mashhoon and Singh [11]. In this paper, they study the case for circular equatorial motion in the exterior Kerr spacetime and compare numerically their calculations with the numerical solution of the extended pole-dipole system in Kerr spacetime given by the MPD equations.

In the MPD equations, the solution of the motion of spinning test particles, it is necessary to consider a spin supplementary condition (SSC) which determines the center of mass of the particle for obtaining the evolution equation. Kyrian and Semerek in their paper [12] consider different spin conditions and compare the different trajectories obtained for various spin magnitudes and conclude that the behaviour of a spinning test particle with different suplementary conditions fixing different representative worldlines. For the numerical integration, they take the case when the spin in orthogonal to the equatorial plane. In a previous paper, they integrated the MPD equations with the Pirani condition ($P_\sigma S^{\mu\sigma} = 0$) [13], and studied the effect of the spin-curvature interaction in the deviations from geodesic motion when the spinning test particles are ejected from the horizon of events of central mass in a meridional plane.

To study the influence of the spin in the gravitomagnetic clock effect, Faruque [14] calculates the first-order correction of the angular velocity analytically with the aim of finding the orbital period both for the prograde period and for the retrograde period of the two spinning test particles. He found that the spin value of the particle reduces the magnitude value of the clock effect. The spin value (S) is fixed and does

not change in the time.

In the last decades, authors such as Kyrian [12], Semerák [13], Plyatsko [15] and Mashhoon [11] worked in the numerical solution of the equations of motion for spinning test particles orbiting around a rotating gravitational field given by the MPD equations. In each case, they performed numerical calculations for a particular case, such as the particle in an equatorial plane or the spin value constant in time. For the scope of this work, the most important contribution will be he numerical solution of the full set of MPD equations without any restrictions on spin orientation. These results will be material for studying the gravitomagnetics effects and for the influence of the spin in Michelson-Morley type experiments.

The formulation of Carter´s equations in order to calculate the system of equations of motion for a test particle in a rotating field derived directly from the Kerr metric using the symmetries of the geometry of a rotating massive body and from the conserved quantities of energy (E), angular momentum (J) and a constant fourth given by Carter (Q).

In the literature, there are papers that use the Carter´s equations to study the motion of spinless test particles in the equatorial plane in a Kerr metric [16],[17]. In particular for Carter´s equations, when the spinless test particle is orbiting in non equatorial planes, there are two particular situations. First, authors as Kheng [18], Teo [19] and Wilkins [20] study the case where the particle is out of the equatorial plane and does not have spin, while Tsoubelis [21], [22] and Stog [23] work on the case where the spinless test particles start from one of the poles of the rotating central mass. We make a numerical comparison from the results obtained by the Carter´s equations with our results given by numerical solution to the full MPD equations.

If one knows the conserved constants, the Killing vector and the covariant derivative of this Killing vector in a point, one can establish a constant relation between

the associated momentum to the conserved quantity and the spin of the test particle in the case when the spinning test particles are in the equatorial plane. With this relation and the Carter´s equations, we will study the particular case when the spin of the particle is parallel to the symmetric axis of the massive rotating body and is orbiting in an equatorial plane. The majority of papers consider the particular case when the value spin is fixed and orthogonal to equatorial plane [24], [25].

One of the purposes of this thesis is to study the gravitomagnetic effects. These effects are derived by the analogy between Coulomb´s law and the Newton´s gravitation law. There is a relationship between the Maxwell´s equations and the linearized Einstein equations. Therefore, our first step will be to linearize the Einstein field equations and compare them with some electromagnetic phenomena. Then, we will take the MPD equations given by Plyastsko *et al.* for a spinning test particle orbiting around a rotating massive body [15]. Since is not possible to find an analytical solution for the set of eleven coupled differential equations, we will give a numerical solution for the case when the spinning test particle orbits in a Kerr metric. The main contribution of this work is to yield the numerical solution for the case of spinning particles around a rotating gravitational field. On the other hand, one finds that the majority of works give the analytical solution for particular cases such as spinless test particles in the Schwarzschild metric and in the equatorial planes or the spin values constricted in the time. We calculate the trajectories of spinning test particles in rotating gravitational fields without restrictions on its velocity and spin orientation. From this work, we will study the gravitomagnetism effects and give an exact numerical solution for the clock effect [26].

Thereafter, we study the effects of spin when a test particle travels in the field of a rotating massive body with the aim of describing the trajectories of test particles in Michelson and Morley type experiments.

The present thesis is structured as follows. It begins with a theoretical chapter which synthesises the basic elements that we will work for studying the motion of spinning test particles around a rotating massive body. In this same chapter, we give an overview of the MPD equations and the Carter´s equations that we will work in this thesis for our numerical calculations.

In the third chapter, we will give the basic structure for describing the trajectories of test particles in a Kerr metric both in the Mathisson-Papapetrou-Dixon equations and in Carter´s equations. We yield the set of equations of motion for the spining test particles when they are orbiting around a rotating massive body.

The fourth chapter is centered on the study of the gravitomagnetism with regard to the study of trajectories of spinning test particles. First of all, we give an overview about the *Gravity Probe B* experiment whose objetive was to detect both the Lense - Thirring effect and the precession of a gyroscope when is orbiting the meridional plane of Earth [27]. NASA launched a satellite which transported four gyroscopes with the aim of measuring the drag of inertial systems and the geodetic effect produced by the gravitational field [28]. Then we study the gravitomagnetic effects given by the rotation of massive bodies and the relationship with spinning test particles. Also, we study the effects by spin in the description of trajectories of test particles around of rotating fields. Finally, we study the Michelson-Morley type experiments with the aim of introducing the influence of stablishing the spin. For this famous experiment, we study the consequences of introducing the spin for the test particle and considering its behavior.

The last chapter is dedicated to the conclusions and outlook of work. We will give a numerical solution both for the MPD equations and for Carter´s equation with the objective of comparing these methods when the two test particles are orbiting around a rotating body in opposite directions. We will compare our results with the

literature and will give our conclusions [14]. Also, we will present a future work with regard to the description of trajectories of spinning test particles when traveling in non-equatorial planes.

Chapter 2

Formulation for the equations of motion

2.1 Introduction

In this chapter, we will consider the effects of the spin for the test particles. In particular we will study the motion of spinning test particles in symmetric axial gravitational fields in the weak field approach. We will use the two different standard formulations by the Mathisson - Papapetrou - Dixon equations (MPD) [10], and the Carter´s equations [6] as starting point of our specific problem. We will extend the MPD formulation by including the spin, obtaining the equations of motion with an explicit spin dependency. On the other hand, we will use the Carter formulation to obtain the specific values for some constants and also to compare the contributions of the final results respect to the already accepted calculations.

In the gravitational field the free particles follow a geodesic. The geodesic is defined as the curve which its tangent vector ($X^\alpha = dx^\alpha/d\lambda$) is parallel transported along the curve, which in terms of its covariant derivative can be written [30] as:

$$\frac{D}{\partial\lambda}\left(\frac{\partial}{\partial\lambda}\right) = \nabla_x X = 0.$$

Using the coordinate basis, $\{\partial/\partial x^\alpha\}$ and $\{dx^\alpha\}$ one obtaines the equation for the geodesics:

$$\frac{d^2x^\alpha}{d\lambda^2} = \Gamma^\alpha_{\beta\gamma}\frac{dx^\beta}{d\lambda}\frac{dx^\gamma}{d\lambda}, \tag{2.1}$$

where $\Gamma^\alpha_{\beta\gamma}$ are the coefficients of connection and λ is an affine parameter. These coefficients are defined in terms of the metric $g_{\mu\nu}$ as

$$\Gamma^\alpha_{\mu\nu} = \frac{1}{2}g^{\alpha\rho}\left(\partial_\nu g_{\rho\mu} + \partial_\mu g_{\rho\nu} - \partial_\rho g_{\mu\nu}\right). \tag{2.2}$$

The test particle follows a geodesic which represents the trajectory in a gravitation field without taking into account any kind of forces.

There are two cases in consideration: first, the test particle has mass, that is, the affine parameter λ is the proper time (τ) and the four velocity $dx^\mu/d\tau$ is normalized as $g_{\mu\nu}\left(dx^\mu/d\tau\right)\left(dx^\nu/d\tau\right) = c^2$. For the second case, the particle does not have mass so that the tangent vector k^μ is null, therefore $g_{\mu\nu}k^\mu k^\nu = 0$.

We will solve the equations of motion for a spinning test particle in a Kerr metric. For this chapter, we define the signature of the metric as (-, -, -,+). This metric in Boyer Lindquist (r, θ, ϕ, t) coordinates is given by [31]

$$\begin{aligned} ds^2 &= -\frac{\rho^2}{\Delta}dr^2 - \rho^2 d\theta^2 - \left[r^2 + a^2 + \frac{2GMr}{c^2\rho^2}a^2\sin^2\theta\right]\sin^2\theta d\phi^2 \\ &\quad + \frac{4GMr}{c^2\rho^2}ac\sin^2\theta dt d\phi + \left(1 - \frac{2GMr}{c^2\rho^2}\right)c^2dt^2, \end{aligned} \tag{2.3}$$

where:

$$\rho^2 = r^2 + a^2 \cos^2 \theta, \tag{2.4}$$

$$\Delta = r^2 - \frac{2GMr}{c^2} + a^2, \tag{2.5}$$

a is the angular momentum of the distribution for unit of mass:

$$a = \frac{J}{Mc}. \tag{2.6}$$

2.2 Equation of linear field

For a given mass distribution and test particles far away from this distribution, the gravitational field is asymptotically Minkowskian; in other words, when one is far away from this distribution, the gravitational force is weak and the gravitational space is a Minkowskian space. Therefore, one can consider under certain conditions that the metric for this mass distribution deviates a little from the Minkowskian metric and one would speak of a relativistic weak gravitational field.

In the approximation of weak gravitational field, we find the approximated solution for the Einstein field equations of the General Relativity Theory; that means, we linearize the gravitational field equations.

2.2.1 Newtonian mechanics

The Newtonian gravitational theory is included in the General Relativity Theory for the conditions of low velocities and weak field:

The velocities are small relative to the speed of light [1]

$$\frac{|\mathbf{u}|}{c} \ll 1 \tag{2.7}$$

and under this condition (2.7) when a particle travels from a point where the gravitational potential is equal zero to a distribution of mass, we have that the gravitational potential Φ is given by

$$\Phi = -\frac{GM}{r}, \tag{2.8}$$

and is called the condition of weak field. This potential must satisfices

$$\frac{2\,|\Phi|}{c^2} \ll 1. \tag{2.9}$$

In this limit we are in the Newtonian gravity [32].

The second condition is the weak field and indepent of time, that is, the temporal variations of field are negligible. In other words, the mass that produces the field is moving slowly.

2.2.2 General Relativity for a weak field

Now, under the approximation of weak field (2.9) the metric can be written as:

$$g_{\mu\nu} = \eta_{\mu\nu} + h_{\mu\nu}, \qquad |h_{\mu\nu}| \ll 1. \tag{2.10}$$

In General Relativity and in the approximation of weak field, one can approach a finite distribution of matter with a small deviation of plane space.

From (2.10) the contravariant components of the metric tensor are given by

[1] Bold characters correspond to vectors in R3

$$g^{\alpha\beta} = \eta^{\alpha\beta} - h^{\alpha\beta}. \tag{2.11}$$

Thus replacing (2.11) in the symbol of Christoffel (2.2) and retaining terms of first order in $h^{\alpha\beta}$ we obtain

$$\Gamma^{\sigma}_{\mu\nu} = \frac{1}{2}\eta^{\alpha\sigma}\left(h_{\alpha\mu,\nu} + h_{\alpha\nu,\mu} - h_{\mu\nu,\alpha}\right). \tag{2.12}$$

We consider a test particle in the gravitational field and free from external forces, so the geodesic equation for the spatial components ($i = 1, 2, 3$) is given by

$$\frac{d^2x^i}{d\tau^2} + \Gamma^{i}_{\alpha\beta}\frac{dx^a}{d\tau}\frac{dx^\beta}{d\tau} = 0. \tag{2.13}$$

In the approach of low velocities and weak field independent of time, the second term of the left of (2.13) is reduced to

$$\Gamma^{i}_{\alpha\beta}\frac{dx^a}{dt}\frac{dx^\beta}{dt} \simeq c^2\Gamma^{i}_{44}. \tag{2.14}$$

From (2.13) we have

$$\frac{d^2x^i}{dt^2} \simeq -c^2\Gamma^{i}_{44}. \tag{2.15}$$

The connection is showed as

$$\Gamma^{i}_{44} = -\frac{1}{2}h_{44,i}, \tag{2.16}$$

then the geodesic equation is

$$\frac{d^2x^i}{d^2t} = \frac{c^2}{2}\frac{\partial h_{44}}{\partial x^i}. \tag{2.17}$$

Comparing (2.17) with equation of motion (2.1) we have

$$h_{44} = -\frac{2}{c^2}\Phi + \text{cte.} \tag{2.18}$$

In a finite distribution of mass $\Phi \longrightarrow 0$, when $r \longrightarrow \infty$, the metric is asymptotically flat, i.e., $h \longrightarrow 0$ for $r \longrightarrow \infty$. So in the equation (2.18) the constant $cte = 0$.

The g_{44} component of the metric is

$$g_{44} \simeq -1 - 2\frac{\Phi}{c^2}. \tag{2.19}$$

The next step is to write the Einstein field equations in the approximation of weak field and low velocities. For that case the equations are written in terms of h and given by

$$G_{\mu\nu} \equiv R_{\mu\nu} - \frac{1}{2}g_{\mu\nu}R = \frac{8\pi G}{c^4}T_{\mu\nu}, \tag{2.20}$$

and the Ricci tensor is given by

$$R_{\lambda\mu} = \Gamma^{\sigma}_{\sigma\lambda,\mu} - \Gamma^{\sigma}_{\lambda\mu,\sigma} + \Gamma^{\tau}_{\lambda\sigma}\Gamma^{\sigma}_{\mu\tau} - \Gamma^{\tau}_{\lambda\mu}\Gamma^{\sigma}_{\tau\sigma}, \tag{2.21}$$

where the comma represents the partial derivative.

We write the Christoffel symbols (2.2) in terms of $h_{\mu\nu}$ as:

$$\Gamma^{\gamma}_{\mu\nu} = \frac{1}{2}\left[h_{\nu}{}^{\gamma},_{\mu} + h^{\gamma}{}_{\mu,\nu} - h_{\mu\nu}{}^{,\gamma}\right]. \tag{2.22}$$

So the Ricci tensor (2.21), in the approximation of weak field, using the expression (2.22), is given by:

$$R_{\mu\nu} = \frac{1}{2}\left[h_{,\mu\nu} - h_{\nu}{}^{\alpha}{}_{,\mu\alpha} - h_{\mu}{}^{\alpha}{}_{,\nu\alpha} + h_{\mu\nu,\alpha}{}^{\alpha}\right] \tag{2.23}$$

and the curvature scalar becomes:

$$R = \left[h_{,\alpha}{}^{\alpha} - h^{\alpha\beta}{}_{,\alpha\beta}\right]. \tag{2.24}$$

So we replace (2.10), (2.23), and (2.24) in the Einstein tensor (2.20) and we obtain

$$\begin{aligned} & \frac{1}{2}\left[h_{,\mu\nu} - h_{\nu}{}^{\alpha}{}_{,\mu\alpha} - h_{\mu}{}^{\alpha}{}_{,\nu\alpha} + h_{\mu\nu,\alpha}{}^{\alpha}\right] - \frac{1}{2}\left(\eta_{\mu\nu} + h_{\mu\nu}\right)\left[h_{,\alpha}{}^{a} - h^{\alpha\beta}{}_{,\alpha\beta}\right] \\ = \quad & \frac{8\pi G}{c^4} T_{\mu\nu}. \end{aligned} \tag{2.25}$$

We define

$$\overline{h}_{\mu\nu} = h_{\mu\nu} - \frac{1}{2}\eta_{\mu\nu} h, \tag{2.26}$$

where h is defined as: $h = h_{\alpha}{}^{\alpha}$. The equation (2.25) can be expressed as

$$-\overline{h}_{\mu\nu,\alpha}{}^{\alpha} + \eta_{\mu\nu}\overline{h}^{\alpha\beta}{}_{,\alpha\beta} - \overline{h}_{\nu}{}^{\alpha}{}_{,\mu\alpha} - \overline{h}_{\mu}{}^{\alpha}{}_{,\nu\alpha} = \frac{16\pi G}{c^4} T_{\mu\nu}, \tag{2.27}$$

in this equation the first term corresponds to D ´lambertian operator which is defined as

$$\overline{h}_{\mu\nu,\alpha}{}^{\alpha} = \Box\overline{h}_{\mu\nu} = \left(-\partial_t^2 + \partial_x^2 + \partial_y^2 + \partial_z^2\right)\overline{h}_{\mu\nu}. \tag{2.28}$$

If one use the Hilbert gauge or Lorentz gauge, the equation (2.27) is reduced to

$$\overline{h}^{\mu\alpha}{}_{,\alpha} = 0. \tag{2.29}$$

From this gauge the linearized field equations (2.27) take the form of a non-homogeneous wave equation:

$$\Box\overline{h}_{\mu\nu} = -\frac{16\pi G}{c^4}T_{\mu\nu}. \tag{2.30}$$

After finding the relationship between the metric tensor and the potential in the newtonian limit, we obtain a particular solution of (2.30), for a spherical uniform mass distribution with a constant angular velocity. With help of this wave equation, in the approximation of low velocities and weak field, the components of tensor $T_{\mu\nu}$ give the expressions analogous to the Maxwell´s equations.

The delayed solution of the non-homogenous wave, the equation (2.30) can be written as

$$\overline{h}_{\mu\nu}\left(ct, \mathbf{x}\right) = -\frac{4G}{c^4}\int \frac{T_{\mu\nu}\left(ct - \left|\mathbf{x} - \mathbf{x\prime}\right|, \mathbf{x\prime}\right)}{\left|\mathbf{x} - \mathbf{x\prime}\right|} d^3\mathbf{x\prime}, \tag{2.31}$$

where $x^\mu = (ct, \mathbf{x})$. Now for the case stationary, that is, $T^{\mu\nu}{}_{,0} = 0$. In other words, the momentum - energy tensor is constant in time, the solution (2.31) is reduced to:

$$\overline{h}^{\mu\nu}\left(\mathbf{x}\right) = -\frac{4G}{c^4}\int \frac{T^{\mu\nu}\left(\mathbf{x\prime}\right)}{\left|\mathbf{x} - \mathbf{x\prime}\right|} d^3\mathbf{x\prime}. \tag{2.32}$$

A particular case is the non-relativistic stationary source, where the velocity u of any particle is small compared with the density of energy [35].

In any coordinated system x^μ, where the four velocity is u^μ, the contravariant components of tensor are given by

$$T^{\mu\nu} = \rho u^\mu u^\nu, \tag{2.33}$$

where ρ is the proper density of fluid and u^μ is the four velocity of fluid which is

defined as: $u^{\mu} = \gamma_u (c, \mathbf{u})$. In the limit of low velocities the Lorentz factor $\gamma_u = (1 - u^2/c^2)^{-1/2} \approx 1$. Therefore the components of the metric tensor are

$$T^{ij} = \rho u^i u^j, \qquad T^{4i} = c j^i, \qquad T^{44} = \rho c^2. \tag{2.34}$$

From the relation $|T^{ij}| / |T^{44}| \sim u^2/c^2$, thus $T^{ij} \approx 0$ up to the order of approximation written above. Let be defined the scalar gravitational potential Φ and the potential gravitational vector A^i, independent of time as

$$\Phi (\mathbf{x}) \equiv -G \int \frac{\rho (\mathbf{x}')}{|\mathbf{x} - \mathbf{x}\prime|} d^3\mathbf{x}', \tag{2.35}$$

$$A^i (\mathbf{x}) \equiv -\frac{4G}{c^2} \int \frac{\rho (\mathbf{x}') u^i (\mathbf{x}')}{|\mathbf{x} - \mathbf{x}\prime|} d^3\mathbf{x}'. \tag{2.36}$$

Thus the solution for (2.32), in the linearized equations, can be written as

$$\overline{h}^{ij} = 0, \qquad \overline{h}^{4i} = \frac{A^i}{c}, \qquad \overline{h}^{44} = \frac{4\Phi}{c^2}. \tag{2.37}$$

The corresponding components of $h^{\mu\nu}$ are given by $h^{\mu\nu} = \overline{h}^{\mu\nu} - \frac{1}{2}\eta^{\mu\nu}\overline{h}$. The result (2.37) implies that $\overline{h} = \overline{h}^{44}$ and the components will be

$$h_{11} = h_{22} = h_{33} = h_{44} = \frac{2\Phi}{c^2}, \qquad h_{4i} = \frac{A_i}{c}. \tag{2.38}$$

From the line element

$$ds^2 = g_{\mu\nu} dx^{\mu} dx^{\nu}$$

and in the approximation of weak field, where the metric is given by $g_{\mu\nu} = \eta_{\mu\nu} + h_{\mu\nu}$ we have

$$g_{ij} = -1 + \frac{2\Phi}{c^2} g_{4i} = \frac{A_i}{c}, \qquad g_{44} = 1 + \frac{2\Phi}{c^2},$$

thus the line element is

$$ds^2 = -\left(1 - \frac{2\Phi}{c^2}\right)\delta_{ij}dx^i dx^j + \frac{4}{c}\left(\mathbf{A}\cdot d\mathbf{x}\right)dt + c^2\left(1 + \frac{2\Phi}{c^2}\right)dt^2. \tag{2.39}$$

Now the aim is to find the analogy between the linearized Einstein field equations and the electromagnetism. We already found that the elements of tensor h are

$$h^{11} = h^{22} = h^{33} = h^{44} = \frac{2\Phi}{c^2}, \qquad h^{4i} = \frac{A^i}{c}, \qquad h^{ij} = 0 \text{ if } i \neq j, \tag{2.40}$$

where Φ and $\mathbf{A}$ are defined as the gravitational scalar and the potential vector respectively. Now let´s consider the time independent Maxwell equations

$$\boldsymbol{\nabla}^2\Phi = -\frac{\rho}{\epsilon_0} \qquad y \qquad \nabla^2\mathbf{A} = -\mu_0\mathbf{j}$$

and take into account the following identifications [44]

$$\epsilon_0 \longleftrightarrow -\frac{1}{4\pi G} \qquad \text{y} \qquad \mu_0 \longleftrightarrow -\frac{16\pi G}{c^2}, \tag{2.41}$$

we can obtain the linerarized field equations:

$$\boldsymbol{\nabla}^2\Phi = 4\pi G\rho \qquad \text{y} \qquad \nabla^2\mathbf{A} = \frac{16\pi G}{c^2}\mathbf{j}, \tag{2.42}$$

where $\mathbf{j} \equiv \rho\mathbf{v}$ is the density (or density of mass current). These equations, time independent, have the solutions (2.35 and 2.36).

So we have the gravitomagnetic and gravitoelectric fields [33] :

$$\mathbf{B} = \boldsymbol{\nabla} \times \mathbf{A} \qquad \text{y} \qquad \mathbf{E} = -\boldsymbol{\nabla}\Phi - \frac{1}{c}\frac{\partial}{\partial t}\left(\mathbf{A}\right). \tag{2.43}$$

Using the equations (2.42), we verify $\mathbf{E}$ and $\mathbf{B}$ fields are relationed to the Maxwell´s equations as

$$\begin{aligned} \boldsymbol{\nabla} \cdot \mathbf{E} &= -4\pi G\rho & \boldsymbol{\nabla} \cdot \frac{1}{2}\mathbf{B} = 0 \\ \boldsymbol{\nabla} \times \mathbf{E} &= -\frac{1}{c}\frac{\partial}{\partial t}\left(\frac{1}{2}\mathbf{B}\right) & \boldsymbol{\nabla} \times \mathbf{B} = \frac{1}{c}\frac{\partial}{\partial t}\mathbf{E} - \frac{4\pi G}{c}\mathbf{j}. \end{aligned} \tag{2.44}$$

The same as in electromagnetism, we must postulate, in addition the Lorentz force for describing this motion. In the last section, we wrote the equation of motion for the test particle in a gravitational field is the geodesic equation:

$$\ddot{x}^{\sigma} + \Gamma^{\sigma}_{\mu\nu}\dot{x}^{\mu}\dot{x}^{\nu} = 0, \tag{2.45}$$

the points indicate the differentation in regard to the proper time τ of the particle. It is taken a small velocity v and the relation $\gamma_v = \left(1 - v^2/c^2\right)^{-\frac{1}{2}} \approx 1$. Writing the position $x^{\mu} = (ct, \mathbf{x})$, the four velocity of the particle is given by [35]

$$\dot{x}^{\mu} = \gamma_v \left(c, \mathbf{v}\right) \approx \left(c, \mathbf{v}\right).$$

Now we replace the derivatives with respect to t. Therefore, the spatial components of (2.45) are written as

$$\begin{aligned}\frac{d^2x^i}{dt^2} &\approx -\left(c^2\Gamma^i_{00} + 2c\Gamma^i_{oj}v^j + \Gamma^i_{ij}v^iv^j\right) \\ &\approx -\left(c^2\Gamma^i_{00} + 2c\Gamma^i_{oj}v^j\right), \end{aligned} \tag{2.46}$$

where we had canceled spatials terms because their reason with respect to temporal term $c^2\Gamma^i_{44}$ is order to v^2/c^2. To first order of gravitational field $h_{\mu\nu}$, the conecction coefficients are given by (2.22). So we take (2.46) and remembering that $h^{ij} = 0$, we obtain

$$\begin{aligned}\frac{d^2x^i}{dt^2} &\approx c\left(h_{4j},^i - h^i_{4,j}\right)v^j - c^2h^i_{4,4} + \frac{1}{2}c^2h_{44},^i \\ &= -c\delta^{ik}\left(h_{4j,k} - h_{4k,j}\right)v^j - c^2\delta^{i\sigma}h_{i4,4} - \frac{1}{2}c^2\delta^{ij}h_{44,j}. \end{aligned} \tag{2.47}$$

Replacing the values of (2.40) in the previous equation, the expression for the motion is written as

$$\frac{d^2\mathbf{x}}{dt^2} \approx -\boldsymbol{\nabla}\Phi - \frac{1}{c}\frac{\partial}{\partial t}\left(\mathbf{A}\right) + \mathbf{v}\times\left(\boldsymbol{\nabla}\times\mathbf{A}\right).$$

Then, we use (2.43) and obtain the Lorentz force for the case gravitational as:

$$\frac{d^2\mathbf{x}}{dt^2} \approx \mathbf{E} + \mathbf{v}\times\mathbf{B}, \tag{2.48}$$

for particles that are moving very slowly in the gravitational field of a stationary mass distribution.

Now then, we can conclude that the Gravitomagnetic Effects (GM) are generated by a mass current, in analogy with the features of magnetism made for a mass current.

In the literature [33], [34] can be found a parallel between the problems characterized by Maxwell´s Equations and the linearized Einstein field Equations. We will discuss about this issue in the next sections.

2.3 Linearized Kerr Metric

We take the Kerr metric in the Boyer Lindquist coordinates (r, θ, ϕ, t) as in eq. (2.3). This metric describes the spacetime geometry outside a rotating body. Also we can approach the geometry far away from the source with the linearization of this metric. Let´s define the lenghts, a and MG/c^2, which are small compared to the distance (r) from the central body to the spinning test particle, that is, $a/r \ll 1$ and $MG/c^2 r \ll 1$. Then Kerr Metric can be linearized in a/r and $MG/c^2 r$ [35] and be written in the following way:

$$g_{\mu\nu} \approx \begin{pmatrix} -1 & 0 & 0 & 0 \\ 0 & -r^2 & 0 & 0 \\ 0 & 0 & -r^2 \sin^2\theta & 0 \\ 0 & 0 & 0 & 1 \end{pmatrix} + \begin{pmatrix} -\frac{2MG}{c^2 r} & 0 & 0 & 0 \\ 0 & 0 & 0 & 0 \\ 0 & 0 & 0 & \frac{2GMa\sin^2\theta}{cr} \\ 0 & 0 & \frac{2GMa\sin^2\theta}{cr} & -\frac{2MG}{c^2 r} \end{pmatrix}. \tag{2.49}$$

This linealization divides the metric two parts, in a flat part and an additive perturbation part, allowing the interpretation to distinguish for the flat part, an extra like effective potential

$$g_{\mu\nu} \approx \eta_{\mu\nu} + h_{\mu\nu} \tag{2.50}$$

where $\eta_{\mu\nu}$ are the components of flat spacetime, and $|h_{\mu\nu}| \ll 1$ are the perturbative elements. Therefore the line element for the Kerr Metric in the limit of weak field [35] will be given by

$$\begin{aligned} ds^2 &= -\left(1 + \frac{2GM}{c^2 r}\right) dr^2 - \left(r^2 d\theta^2 + r^2 \sin^2\theta d\phi^2\right) \\ &\quad + \frac{4GMa}{cr} \sin^2\theta d\phi dt + c^2 \left(1 - \frac{2GM}{c^2 r}\right) dt^2. \end{aligned} \tag{2.51}$$

where the $g_{t\phi}$ component is called the gravitomagnetic potential.

This metric is useful for calculating the General Relativity effects due to the rotation of the Earth, or in astrophysical situations, where the gravitational field is weak.

The gravitomagnetic term generally is refered to the set of gravitational phenomena with relation to the orbiting test particles, precession of gyroscopes, motion of clocks and atoms, and the propagation of electromagnetic waves which in the system of General Relativity Einstein Theory comes from distributions of matter and energy no static [34]. In the approximation of weak field and low velocities, the Einstein field equations (2.20), are linearized and it is found the analogy with the Maxwell´s equations for electromagnetism. As a consequence, a gravitomagnetic field $\overrightarrow{B}_g$, induced for the components no diagonal g_{4i}, $i = 1, 2, 3$ of the metric of space time related with mass-energy currents are present. A particular case is given when the particle is far away from a rotating body with angular momentum $\overrightarrow{J}$, in consequence the gravitomagnetic field can be written as

$$\overrightarrow{B}_g(\overrightarrow{r}) = \frac{G}{cr^3}\left[\overrightarrow{J} - 3\left(\overrightarrow{J}\cdot\widehat{r}\right)\widehat{r}\right], \tag{2.52}$$

where G is the newtonian gravitational constant. This concerns, for instance, to a test particle that is moving with a velocity $\overrightarrow{v}$. The acceleration is given by

$$\overrightarrow{A}_{GM} = \left(\frac{\overrightarrow{v}}{c}\right) \times \overrightarrow{B}_g, \tag{2.53}$$

which is the cause of two gravitomagnetic effects: Lense - Thirring Effect and the geodesic precession.

Now we will present the basics for the motion of spinning test particles around a rotating massive body, according to the formulations by MPD equations and Carter´s equations.

2.4 Mathisson - Papapetrou - Dixon equations

In order to obtain the MPD equations of motion, we take the momentum energy symmetric tensor for a mass distribution ($T^{\alpha\beta}$), which satisfies the equation of continuity

$$\nabla_\beta T^{\alpha\beta} = 0. \tag{2.54}$$

Using the geometrized units ($c = G = 1$), and the greek indices running from $1 - 4$.

This approximation works out for very small bodies, allowing for the neglect of the influence of other bodies on the body of interest. This body is normally called *a test particle*. As a consequence, the dimensions of the test particle are very small compared to the characteristic lenght of gravitational field. In this way, the particle

describes a narrow world tube (M) in a four dimensional space-time (Figure 2.1). Inside this tube, the line l represents the motion of the particle [7]. In this thesis, we take the particular spin condition which fixes a center of mass and establishs an interaction between the intrinsic angular momentum and the gravitational field. A world tube is formed by all possible centroids [12].

Now we define the linear and angular momentum for the test particle, which is described for a momentum-energy symmetric tensor. For a test particle, described by a tensor $T^{\alpha\beta}$, the radius of a world tube W is not zero (Figure 2.1). This tube is spread in the time, both in the past and in the future, but it is bounded spatially. It is assumed that spacetime accepts isometries that are described by the Killing vector ξ_β such that

$$\nabla_{(\alpha}\xi_{\beta)} = 0, \tag{2.55}$$

and the equation (2.55) shows that

$$\nabla_\alpha \left(\xi_\beta T^{\alpha\beta}\right) = \left(\nabla_\alpha \xi_\beta\right) T^{\alpha\beta} + \xi_\beta \left(\nabla_\alpha T^{\alpha\beta}\right) = 0. \tag{2.56}$$

Integrating the expression (2.56) on a volume M which includes a part of world tube W, and considering an arbitrary like time surface, and two spacelike hypersurfaces Σ_1 and Σ_2, the integral takes the form [9]

$$\int_M \nabla_\alpha \left(\xi_\beta T^{\alpha\beta}\right) \sqrt{-g} d^4x = 0, \tag{2.57}$$

which can be written as

$$\int_M \partial_\alpha \left(\sqrt{-g}\xi_\beta T^{\alpha\beta}\right) d^4x = 0. \tag{2.58}$$

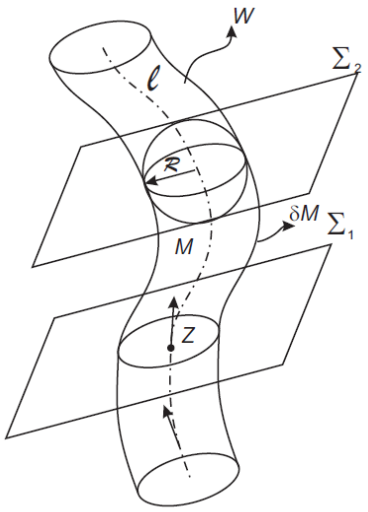

Figure 2.1: World tube line of the spinning test particle

Now writing each part that defines the surface M

$$\int_{\Sigma_2 \cap M} \xi_\beta T^{\alpha\beta} d\Sigma_\alpha + \int_{\Sigma_1 \cap M} \xi_\beta T^{\alpha\beta} d\Sigma_\alpha + \int_{\partial M} \xi_\beta T^{\alpha\beta} d\Sigma_\alpha = 0. \tag{2.59}$$

The last term vanishes because $T^{\alpha\beta}$ is zero in ∂M and the others two terms can be restricted to $\Sigma_\alpha \cap W$ for the same reason. So,

$$\int_{\Sigma_2 \cap M} \xi_\beta T^{\alpha\beta} d\Sigma_\alpha = -\int_{\Sigma_1 \cap M} \xi_\beta T^{\alpha\beta} d\Sigma_\alpha. \tag{2.60}$$

Therefore,

$$\int_{\Sigma} \xi_\beta T^{\alpha\beta} d\Sigma_\alpha = C, \tag{2.61}$$

is a constant of motion, independient of the hypersurface.

Consider a general space time $\widetilde{M}$ and let be $x(\lambda, \gamma)$ a family parametric of geodesics in this space time, where γ classifies the geodesics and λ is the affine parameter along of each geodesic. One has

$$\dot{x}^{\alpha} := \frac{\partial x^{\alpha}}{\partial \lambda} \qquad \text{and} \qquad V^{\alpha} := \frac{\partial x^{\alpha}}{\partial \gamma}, \tag{2.62}$$

where $\dot{x}^{\alpha}$ is the tanget vector to the geodesic and V^{α} is the deviation vector. Then, $V^{\alpha}(\lambda, \gamma)$ satisfies the deviation equation of the geodesic for each value γ [10]

$$\frac{D^2 \xi^{\alpha}}{d\lambda^2} + R^{\alpha}{}_{\beta\gamma\delta} \dot{x}^{\beta} \dot{x}^{\gamma} \xi^{\delta} = 0. \tag{2.63}$$

A solution for this equation is determined by the value of ξ^{α} and $D\xi^{\alpha}/d\lambda$ in any fixed value of λ. Now one chooses any fixed point of z and supposes that the values of ξ_{α} and $\nabla_{[\alpha}\xi_{\beta]}$ are given in z. One obtains

$$\frac{D\xi_{\alpha}}{d\lambda} = \dot{x}^{\beta} \nabla_{[\beta}\xi_{\alpha]}. \tag{2.64}$$

Now, in the definition of world function, let us have $z \equiv x(\lambda_0 = 0)$ and $x \equiv x(\lambda_0 = \lambda)$. But for the reduced expression given by Dixon [10], σ^{κ} is the derivative of the world function σ at the point $z(\gamma)$, as

$$\sigma^{\kappa} = -\lambda \dot{x}^{\kappa} \qquad \text{y} \qquad \sigma^{\alpha} = \lambda \dot{x}^{\alpha}, \tag{2.65}$$

one obtains

$$\sigma^{\kappa}(z(v), x(\lambda, \gamma)) = -\lambda \dot{x}^{\kappa}(0, \gamma), \tag{2.66}$$

where $z(v) := x(0, \gamma)$. We derive (2.66) respect to γ and as the differentiation works in each term separately, we have

$$\sigma^{\kappa}{}_{\varphi} V^{\varphi} + \sigma^{\kappa}{}_{\alpha} V^{\alpha} = -\lambda \frac{D\dot{x}^{\kappa}}{d\gamma} \tag{2.67}$$

and from (2.62) we obtain

$$\frac{D\dot{x}^{\kappa}}{d\gamma} = \frac{DV^{\kappa}}{d\lambda}. \tag{2.68}$$

It defined $(\sigma^{\alpha}_{.\kappa})^{-1}$ as the inverse of the matrix $\sigma^{\kappa}_{.\alpha}$, therefore

$$(\sigma^{\alpha}{}_{\kappa})^{-1}\,\sigma^{\kappa}{}_{\beta} = A^{\alpha}_{\beta}, \tag{2.69}$$

where A^{α}_{β} is the unit tensor. Then (2.67) with (2.68) one has

$$V^{\alpha} = (\sigma^{\alpha}{}_{\varphi})^{-1}\,\sigma^{\varphi}{}_{\kappa}V^{\kappa} - \lambda\,(\sigma^{\alpha}{}_{\kappa})^{-1}\,\frac{DV^{\kappa}}{d\lambda}. \tag{2.70}$$

The last equation is the formal solution of the deviation equation of the geodesic (2.63). Now we define the bitensors as

$$K^{\alpha}_{.\kappa} = (\sigma^{\alpha}{}_{\varphi})^{-1}\,\sigma^{\varphi}{}_{\kappa} \qquad \text{and} \qquad H^{\alpha}{}_{\kappa} = -\,(\sigma^{\alpha}{}_{\kappa})^{-1}\,; \tag{2.71}$$

therefore the equation (2.70) can be expressed as

$$V^{\alpha} = K^{\alpha}{}_{\kappa}V^{\kappa} - \lambda H^{\alpha}{}_{\kappa}\frac{DV^{\kappa}}{d\lambda}. \tag{2.72}$$

If we apply the last equation to the case where ξ_{α} is a Killing field vector using (2.64) and (2.66) we obtain

$$\xi_{\alpha} = K_{\alpha}{}^{\kappa}\xi_{\kappa} + H_{\alpha}{}^{\kappa}\sigma^{\varphi}\nabla_{[\kappa}\xi_{\varphi]}. \tag{2.73}$$

This expression is acceptable for all x in the neighbourhood of z, and is explicit the setting of ξ_{α} for the values of the Killing field vector ξ_{α} and the covariant derivative $\nabla_{[\kappa}\xi_{\gamma]}$ in a point. If one integrates the last Killing vector (2.73), with the expression (2.61) one obtains

$$\int_{\Sigma}\left(K_{\alpha}\ {}^{\kappa}\xi_{\kappa}+H_{\alpha}\ {}^{\kappa}\sigma^{\lambda}\nabla_{[\kappa}\xi_{\lambda]}\right)T^{\alpha\beta}d\Sigma_{\beta}=C. \tag{2.74}$$

Here $\xi_{\kappa}=\xi_{\kappa}(z)$ and $\nabla_{[\kappa}\xi_{\lambda]}=\nabla_{[\kappa}\xi_{\lambda]}(z)$, z is a fixed arbitrary point. We define the linear and angular momentum as

$$p^{\kappa}(z,\Sigma) \equiv \int_{\Sigma}K_{\alpha}\ {}^{\kappa}T^{\alpha\beta}d\Sigma_{\beta}, \tag{2.75}$$

$$S^{\kappa\lambda}(z,\Sigma) \equiv 2\int_{\Sigma}H_{\alpha}\ {}^{[\kappa}\sigma\ {}^{\lambda]}T^{\alpha\beta}d\Sigma_{\beta}, \tag{2.76}$$

where p^{κ} is the linear momentum and $S^{\kappa\lambda}$ is the spin tensor. There exists in each point z a only four vector u such that u and $p(x,u)$ are collinear [36]

$$u^{[\mu}p^{\nu]}(z,u)=0, \tag{2.77}$$

where [ ] means antisymmetrization. On the other hand, there exists a only world line liketime $z^{\mu}(\lambda)$ that satisfies [36]

$$p_{\mu}(z)\,S^{\mu\nu}(z)=0,$$

this world line is called the center of mass of body.

The constant (2.74) can be written as

$$C=p^{\kappa}(z,\Sigma)\,\xi_{\kappa}+\frac{1}{2}S^{\kappa\gamma}(z,\Sigma)\,\nabla_{[\kappa}\xi_{\gamma]}. \tag{2.78}$$

Since the definitions p^{κ} and $S^{\kappa\lambda}$ do not depend on the Killing vector fields, the definitions can be used for a arbitrary space time without any symmetry. However,

when there exists isommetries in the space time, C gives a linear combination of linear momentum and angular moment which is constant. So we have [37]

$$\frac{D}{d\lambda}\left[p^{\kappa}\left(z,\Sigma\right)\xi_{\kappa}+\frac{1}{2}S^{\kappa\gamma}\left(z,\Sigma\right)\nabla_{[\kappa}\xi_{\gamma]}\right]=0, \tag{2.79}$$

which can be explicit as

$$\frac{Dp^{\kappa}}{d\lambda}\xi_{\kappa}+p^{\kappa}\frac{D}{d\lambda}\xi_{\kappa}+\frac{1}{2}\left(\frac{DS^{\kappa\gamma}}{d\lambda}\nabla_{[\kappa}\xi_{\gamma]}+S^{\kappa\lambda}\frac{D}{d\lambda}\nabla_{[\kappa}\xi_{\gamma]}\right)=0. \tag{2.80}$$

From (2.55) we have $\frac{D}{d\lambda}\xi_{\kappa}=v^{\mu}\nabla_{[\mu}\xi_{\kappa]}$ with $v^{\mu}\equiv\frac{dz^{\mu}}{d\lambda}$, which it defines the tangent vector to world line $z^{\mu}\left(\lambda\right)$; and given that the Killing field vectors satisfies

$$\nabla_{\alpha}\nabla_{\beta}\xi_{\gamma}=R_{\beta\gamma\alpha\delta}\xi^{\delta}, \tag{2.81}$$

so the expression (2.80) can be written as

$$\frac{D}{d\lambda}C=\xi_{\kappa}\left[\frac{Dp^{\kappa}}{d\lambda}+\frac{1}{2}S^{\delta\gamma}u^{\mu}R_{\delta\gamma\mu}{}^{\kappa}\right]+\frac{1}{2}\nabla_{[\kappa}\xi_{\gamma]}\left[\frac{DS^{\kappa\gamma}}{d\lambda}-2p^{[\kappa}u^{\gamma]}\right]=0. \tag{2.82}$$

This equation has a solution for all Killing field vector if each term in the brackets vanishes separately. These terms are defined both the total force and total torque acting on a body [5],

$$F^{\kappa} \equiv \frac{Dp^{\kappa}}{d\lambda}+\frac{1}{2}S^{\delta\gamma}u^{\mu}R^{\kappa}_{\delta\gamma\mu} \tag{2.83}$$

$$L^{\kappa\gamma} \equiv \frac{DS^{\kappa\gamma}}{d\lambda}-2p^{[\kappa}u^{\gamma]}. \tag{2.84}$$

With these definitions one can write (2.82) as

$$\xi_\kappa F^\kappa + \frac{1}{2}\nabla_{[\kappa}\xi_{\gamma]}L^{\kappa\gamma} = 0. \tag{2.85}$$

These two definitions (2.83) and (2.84) can be generalized to arbitrary space time, since they do not depend on Killing vectors. But in a general space time, the higher multipolar momenta contribute to the force and to the torque. The expression (2.85) express the conection between the integrals of motion and the isommetries of space-time.

We take the particular case for a test particle, in this case the force and the torque are zero in the equations (2.83) and (2.84); therefore these equations are reduced to

$$\frac{Dp^\kappa}{d\lambda} = -\frac{1}{2}S^{\delta\gamma}u^\mu R^\kappa_{\delta\gamma\mu} \tag{2.86}$$

$$\frac{DS^{\kappa\gamma}}{d\lambda} = 2p^{[\kappa}u^{\gamma]}. \tag{2.87}$$

For our study, we take the pole-dipole approximation which deals with the equations of motion of a spinning test particle only including the mass monopole and spin dipole. Multipoles of higher orders and non-gravitational effects are ignored. First, when the analysis is restricted to particles whose dynamics is only affected by the monopole moments the motion is simply a geodesic. Second, if it is the dipole moment, the motion corresponds to a test particle with spin and is no longer a geodesic. In this case, the monopole and dipole moments give the kinematic momentum p^μ and the spin tensor $S^{\mu\nu}$ of the body as measured by an observer moving along the reference worldline with velocity V^μ [38].

The set of equations (2.86) and (2.87) has more unknown variables than equations

so the system is undermined. Therefore a spin supplementary condition (SSC) has to be imposed in order to solve the set of equations. This condition is related to the choice of a center of mass whose evolution is described by an observer and where the mass dipole vanishes [39]. When the spinning test particle moves with a constant velocity v the part which moves faster appears to be heavier and the one that moves more slowly appears to be lighter. Therefore, there is a shift of the center of mass Δx compared to an observer with zero-3-momentum. Inside of body size, it is possible to find an observer for whom the reference worldline coincides with the centre of mass. All the possible centroids set up a worldtube whose size is Möller radius.

In the description of the motion of a spinning test particle the tangent vector to the worldline (u^μ) is no longer parallel to the linear momentum p^μ as we know it from geodesic motion. The choice of a supplementary condition is related to the ability to find an expression between u^μ and p^μ [40]. In this case, the rest mass m is not a constant so the kinematical mass is redefined by

$$p_\mu u^\mu = -m \tag{2.88}$$

with respect to the kinematical four-velocity u^μ. Then, the dynamical mass is denoted with regard to the four-momentum p_μ by M which satisfies

$$p_\mu p^\mu = -M^2. \tag{2.89}$$

In this context a dynamical velocity is defined by

$$v^\mu = \frac{p^\mu}{M}. \tag{2.90}$$

In the case, $m = M$, because the tangent vector u^ν is parallel to dynamical four

velocity v^ν when it is the motion of a geodesic.

In general, two conditions are usually imposed. The Mathisson-Pirani supplementary condition is [8], [41]

$$u_\sigma S^{\mu\sigma} = 0. \tag{2.91}$$

In this condition, the observer is comoving with the particle and is in the rest frame of the particle. There is not a unique representative worldline and therefore it is dependent on the observer´s velocity and on the initial conditions. Further, this condition exhibits helical motion in contrast to a straight line in flat spacetime. In the works by Costa *et al.* show that these helical motions are physical motions and have a hidden momentum [42].

Another supplementary condition, it is the Tulczyjew-Dixon condition [43]

$$p_\sigma S^{\mu\sigma} = 0 \tag{2.92}$$

where

$$p^\sigma = mu^\sigma + u_\lambda \frac{DS^{\sigma\lambda}}{ds} \tag{2.93}$$

is the four momentum.

In addition to the MPD equations, we take the Tulczyjew´s condition as supplementary condition (2.92) which implies that $dm/d\tau = 0$. The motion effects induced by this condition must be confined to the worldtube of centroid, that is, the worldtube formed by all the possible positions of the center of mass, as measured by every possible observer [45]. In the the flat spacetime case, it is a tube of radius S/M centered around the center of mass measured in the zero 3-momentum frame.

We contract $S_{\mu\nu}$ in the equation (2.84) and use the condition (2.92), we obtain the magnitude S of spin which it is defined as

$$S^2 = S_\mu S^\mu = \frac{1}{2m^2} S_{\mu\nu} S^{\mu\nu}, \tag{2.94}$$

this is a constant of motion. We obtain the constant too [43]

$$m^2 = p_\mu p^\mu, \tag{2.95}$$

where m is interpreted as the mass of the particle.

In general the four momentum p^μ and the tangent vector u^μ are not colinear. In fact, from the set of equations (2.83), (2.84) and the supplementary condition (2.92), we deduce that [10]

$$p^{[\mu} u^{\nu]} = -\frac{1}{4m} \sqrt{-g} \epsilon^{\mu\nu\lambda\rho} R_{\lambda\alpha\beta\gamma} u^\alpha S^{\beta\gamma} S_\rho, \tag{2.96}$$

where $\epsilon_{\mu\nu\lambda\rho}$ is the antysimmetric tensor and S_ρ is the spin vector which is defined by

$$S_\rho = \frac{1}{2m} \sqrt{-g} \epsilon_{\mu\nu\lambda\rho} p^\mu S^{\nu\lambda}. \tag{2.97}$$

The next step is to parametize the four vector of velocity u^μ and v^μ, with the parameter of proper time τ, as

$$u^\mu(\tau)\, v_\mu(\tau) = 1 \tag{2.98}$$

where v^μ is the four velocity of center of mass, parallel to the line of world l and Dixon calls "dynamic velocity" [43] (2.1). u^μ is called "kinematical velocity" and is perpendicular to hypersurface (Σ).

Now we derive the equation of evolution of $v^\mu(\tau)$ in terms of $u^\mu(\tau)$. For this we take the definition of total four momentum as

$$p^{\mu} = mu^{\mu} - u_{\sigma}\dot{S}^{\mu\sigma}. \tag{2.99}$$

We multiply each one of the sides of the equation for m

$$\begin{aligned} mp^{\mu} &= m^2u^{\mu} - p_{\sigma}\dot{S}^{\mu\sigma}, \\ m^2u^{\mu} - mp^{\mu} &= p_{\sigma}\dot{S}^{\mu\sigma}. \end{aligned} \tag{2.100}$$

We resolve u^{μ}

$$u^{\mu} = \frac{m}{m^2}p^{\mu} + \frac{p_{\sigma}}{m^2}\dot{S}^{\mu\sigma}.$$

It is imposed the restriction $u_{\sigma}S^{\mu\sigma} = 0$, therefore the right part of the equation can be written (2.100) as

$$p_{\sigma}\dot{S}^{\mu\sigma} = -\dot{p}S^{\mu\sigma}. \tag{2.101}$$

We replace this definition in the expression of u^{μ}

$$\begin{aligned} u^{\mu} &= \frac{m}{m^2}mv^{\mu} - \frac{\dot{p}}{m^2}S^{\mu\sigma}, \\ u^{\mu} &= v^{\mu} - \frac{\dot{p}}{m^2}S^{\mu\sigma}. \end{aligned}$$

With the help of the tensor $S^{\mu\nu}$, we find that

$$\left(4m^2 + R_{\rho\alpha\beta\gamma}S^{\alpha\rho}S^{\beta\gamma}\right)\dot{p}_{\sigma}S^{\mu\sigma} = -2mS^{\mu\sigma}R_{\sigma\alpha\beta\gamma}p^{\alpha}S^{\beta\gamma}. \tag{2.102}$$

From the equations (2.100), (2.101), and (2.102) we obtain the following result

$$\begin{aligned} v^{\mu} &= u^{\mu} - \frac{2mS^{\mu\sigma}R_{\sigma\alpha\beta\gamma}p^{\alpha}S^{\beta\gamma}}{m^2\left(4m^2 + R_{\rho\alpha\beta\gamma}S^{\alpha\rho}S^{\beta\gamma}\right)} \\ v^{\mu} &= u^{\mu} - \frac{2mS^{\mu\sigma}R_{\sigma\alpha\beta\gamma}mu^{\alpha}S^{\beta\gamma}}{m^2\left(4m^2 + R_{\rho\alpha\beta\gamma}S^{\alpha\rho}S^{\beta\gamma}\right)} \\ v^{\mu} &= u^{\mu} - \frac{2S^{\mu\sigma}R_{\sigma\alpha\beta\gamma}u^{\alpha}S^{\beta\gamma}}{4m^2 + R_{\rho\alpha\beta\gamma}S^{\alpha\rho}S^{\beta\gamma}} \end{aligned} \tag{2.103}$$

$$v^{\mu} - u^{\mu} = -\frac{1}{2}\left(\frac{S^{\mu\nu}R_{\nu\rho\sigma\kappa}u^{\rho}S^{\sigma\kappa}}{m^2 + \frac{1}{4}R_{\chi\xi\zeta\eta}S^{\chi\xi}S^{\zeta\eta}}\right). \tag{2.104}$$

With this equation (2.104) and the equations (2.86) and (2.87) we determine completely the evolution of the orbit and of the spin for a small spining test particle.

Sometimes it is more useful to work with a spin four-vector S^{μ} than the tensor $S^{\mu\nu}$. The antisymmetry of the spin tensor only allows six independent spin values to be reduced to a four vector. Of course, this four vector S^{μ} depends on the SSC [46] and is defined as (2.97). The measure of the spin divided by the dynamical rest mass, i.e. S/M defines the minimal radius or Möller radius.

When the space-time admits a Killing vector ξ^{υ}, there is a property that includes the covariant derivative and the spin tensor, which gives a constant and is given by the expression [47]

$$p^{\nu}\xi_{\nu} + \frac{1}{2}\xi_{\nu,\mu}S^{\nu\mu} = \text{ constant}, \tag{2.105}$$

where p^{ν} is the linear momentum, $\xi_{\nu,\mu}$ is the covariant derivative of Killing vector, and $S^{\nu\mu}$ is the spin tensor of the particle. In the case of the Kerr metric, there are two Killing vectors, owing to its stationary and axisymmetric nature. In consequence, Eq. (2.105) yields two constants of motion: E, the total energy and J_z, the component of its angular momentum along the axis of symmetry [48].

The next section presents other possible formulation for solving the equation of

motion of a test particle around to a rotating body. This method is called Carter´s equation [6].

2.5 Carter´s equations

Now we present, in a brief form, the Carter´s equations for a particle around a massive rotating body. In a Kerr type metric, the symmetries provide three constant of motion: Energy (E), the angular momentum (J) and the mass (M). In addition, there is another constant which is due to the separability of the Hamilton - Jacobi Equation and is called Q. The Lagrange equation for a Kerr metric gives immediatelly the first integrals of t and φ. For the others two integrals for (r) and (θ) are obtained for a separable solution of the Hamilton - Jacobi equation [49]. The set of equations is given by [23]

$$\begin{aligned}
\Sigma\dot{t} &= a\left(J - aE\sin^2\theta\right) \\
&\quad + \frac{\left(r^2+a^2\right)\left[E\left(r^2+a^2-aJ\right)\right]}{\Delta}, \qquad (2.106)\\
\Sigma\dot{r} &= \pm R = \pm\left\{\begin{array}{c} \left[E\left(r^2+a^2\right)\mp aJ\right]^2 \\ -\Delta\left[r^2+Q+\left(J\mp aE\right)^2\right] \end{array}\right\}^{1/2}, \qquad (2.107)\\
\Sigma\dot{\theta} &= \pm\Theta = \pm\left\{Q-\cos^2\theta\left[a^2\left(1-E^2\right)+\frac{J^2}{\sin^2\theta}\right]\right\}^{1/2}, \qquad (2.108)\\
\Sigma\dot{\phi} &= \frac{J}{\sin^2\theta} - aE + \frac{a}{\Delta}\left[E\left(r^2+a^2\right)-aJ\right], \qquad (2.109)
\end{aligned}$$

where J, E and Q are constants and

$$\Sigma := r^2 + a^2 \cos^2 \theta, \tag{2.110}$$

$$\Delta := r^2 + a^2 - 2Mr,$$

M and $a = J/M$ are the mass and specific angular momentum of the central source.

The Carter´s constant (Q) is a conserved quantity of the particle in free fall around of rotating massive body. This quantity affects the latitudinal motion of the particle and is related with the angular momentum in the direction θ. From (2.108) one analyzes that in the equatorial plane, the relation between Q and the motion in θ is given by

$$\Sigma \dot{\theta}^2 = Q \tag{2.111}$$

When $Q = 0$ correspondes to equatorial orbit and for the case when $Q \neq 0$ one has a non-equatorial orbit.

In the next section, we find that when there are isommetries in the space time, there exist two constants (2.78) that relate the linear and angular momenta.

Chapter 3

Trajectories of test particles in a Kerr metric

In this chapter, we study the set of equations of motion for test particles with spin and without spin, in a Kerr metric [50], [51]. For the scope of our work, in the first formulation (MPD), we used both the Christoffel symbols for a Kerr metric and the values of the curvature tensor [1]. In the second formulation, Carter originally showed that the first integrals of the equations of motion have four constants of motion [52]. We will consider both spinless test particles and spinning test particles, using not only the first formulation (MPD), but also the second formulation (Carter) to be able to compare explicity the respective trajectories (with spin and without spin of the test particle), and study their similarities and discrepancies.

In the literature one can find many works that study all these issues, however most of them are focused on restricted orbits on the equatorial plane of the central mass [53] and only for spinless test particles. We will take these formulations (MPD and Carter) for two different cases. In the first case, we study the equation of motion of spinless test particles. The second case regards to intrinsic spin, that is, with test

particles in rotation [54]. In the literature we found works both for one formulation and for the other, but these works study especially orbits in the equatorial plane of the central mass [55]. One of the main contributions of this work is to include spinning test particles in this framework particulary calculating the equations of motions for spinning test particles out of the equatorial plane.

In this chapter we will present in the first section the first formulation (MPD) for the spinning test particles in an explicit schematic form. This schematic form for the set of equations of MPD is not restricted to a particular metric [56]. We take the Kerr metric which describes the space time ot a rotating massive body. The study of this kind of metric will give us elements to describe the phenomena asociated with gravitomagnetic effects such as Lense-Thirring effect or the clock effect among others [57].

Also, in this chapter, we will study the Carter´s equations. This formulation describes the spinless test particles orbiting in a rotating field. We take this description because we will numerically compare the trajectories of geodesics (Carter) with the trajectories of spinning test particles (MPD). We will take specially both the coordinate time (t) and the cartesian coordinates (x, y, z) for the two cases: trajectories of spinless and spinning test particles. Theses parameteres are a good guide for describing the gravitomagnetic effects in rotating massive bodies.

3.1 Mathisson - Papapetrou - Dixon equations

Given the equations of motion for a test spinning body sufficiently small (Eqs. 2.86 and 2.87), we take the case when the test particles are orbiting a Kerr metric.

According to R.M. Plyatsko *et al.* [58] the full set of the exact MPD equations for the motion of a spinning test particle in the Kerr field. The signature used

here is $(-,-,-,+)$ and the coordinates are (r,θ,φ,t). Moreover the dimensionless quantities are introduced y_i with particle´s coordinates by

$$y_1 = \frac{r}{M}, \qquad y_2 = \theta, \qquad y_3 = \varphi, \qquad y_4 = \frac{t}{M}, \tag{3.1}$$

for its 4-velocity with respect to the proper time s

$$y_5 = u^1, \qquad y_6 = Mu^2, \quad y_7 = Mu^3, \quad y_8 = u^4, \tag{3.2}$$

and the spatial spin components [59]

$$y_9 = \frac{S_1}{mM}, \qquad y_{10} = \frac{S_2}{mM^2}, \qquad y_{11} = \frac{S_3}{mM^2}. \tag{3.3}$$

In addition, they introduce another dimensionless quantities in regard to the proper time s and the constant of motion E, J_z

$$x = \frac{s}{M}, \qquad \widehat{E} = \frac{E}{m}, \quad \widehat{J} = \frac{J_z}{mM}. \tag{3.4}$$

The set of the MPD equations for a spinning particle in the Kerr field is given by eleven equations. The four first equations are

$$\dot{y_1} = y_5, \qquad \dot{y_2} = y_6, \qquad \dot{y_3} = y_7, \qquad \dot{y_4} = y_8, \tag{3.5}$$

where a dot denotes the usual derivative with respect to x.

The fifth equation is given by the first three equations of (2.86) with the indexes $\lambda = 1,2,3$. Also the set of equations (2.87) has three independent differential equations and the condition (2.91) we obtain the relation between $S^{\lambda\nu}$ and u_μ. The result is multiplied by $S_{1,}S_2, S_3$ and taking the relationships: $S^{i4} = \frac{u_k}{u_4}S^{ki}$ and

$S_i = \frac{1}{2u_4}\sqrt{-g}\varepsilon_{ikl}S^{kl}$, we obtain

$$mS_i\frac{Du^i}{ds} = -\frac{1}{2}u^\pi S^{\rho\sigma}S_j R^j_{\pi\rho\sigma} \tag{3.6}$$

which can be written as

$$y_9\dot{y}_5 + y_{10}\dot{y}_6 + y_{11}\dot{y}_7 = A - y_9Q_1 - y_{10}Q_2 - y_{11}Q_3 \tag{3.7}$$

where

$$Q^i = \Gamma^i_{\mu\nu}u^\mu u^\nu, \qquad A = \frac{u^\beta}{\sqrt{-g}}u_4\epsilon^{i\rho\sigma}S_iS_jR^j_{\beta\rho\sigma}. \tag{3.8}$$

In other words, we worked out the MPD equations given by Plyatsko *et al.* [15] under the Pirani - Mathisson spin supplementary condition (2.91). This option brings some physical features for the trajectory of a spinning test particle that we shall explain later.

The sixth equation is given by

$$u_\nu\frac{Du^\nu}{ds} = 0 \tag{3.9}$$

which can be written as

$$p_1\dot{y}_5 + p_2\dot{y}_6 + p_3\dot{y}_7 + p_4\dot{y}_8 = -p_1Q_1 - p_2Q_2 - p_3Q_3 - p_4Q_4 \tag{3.10}$$

where

$$p_\alpha = u_\alpha = g_{\alpha\mu}u^\mu. \tag{3.11}$$

The seventh equation is given by

$$E = P_4 - \frac{1}{2} g_{4\mu,\nu} S^{\mu\nu} \tag{3.12}$$

which can be written as

$$c_1 \dot{y}_5 + c_2 \dot{y}_6 + c_3 \dot{y}_7 = C - c_1 Q_1 - c_2 Q_2 - c_3 Q_3 + \ \widehat{E} \tag{3.13}$$

where

$$\begin{aligned} c_1 &= -d g_{11} g_{22} g_{44} u^2 S_3 - d \left(g_{34}^2 - g_{33} g_{44} \right) g_{11} u^3 S_2 \\ c_2 &= d g_{11} g_{22} g_{44} u^1 S_3 + d \left(g_{34}^2 - g_{33} g_{44} \right) g_{22} u^3 S_1 \\ c_3 &= d \left(g_{34}^2 - g_{33} g_{44} \right) g_{11} u^1 S_2 - d \left(g_{34}^2 - g_{33} g_{44} \right) g_{22} u^2 S_1 \end{aligned} \tag{3.14}$$

$$C = g_{44} u^4 - d g_{44} u^4 g_{43,2} S_1 + d \left(g_{44} u^4 g_{43,1} - g_{33} u^3 g_{44,1} \right) S_2 + d g_{22} u^2 g_{44,1} S_3 \tag{3.15}$$

$$d = \frac{1}{\sqrt{-g}}$$

where $-g$ is the determinant of the metric.

The eighth equation is given by

$$J_z = -P_3 + \frac{1}{2} g_{3\mu,\nu} S^{\mu\nu} \tag{3.16}$$

which can be written as

$$d_1\dot{y}_5 + d_2\dot{y}_6 + d_3\dot{y}_8 = D - d_1Q_1 - d_2Q_2 - d_3Q_4 - \widehat{J} \tag{3.17}$$

where

$$\begin{aligned}
d_1 &= -dg_{11}g_{22}g_{34}u^2S_3 + dg_{11}g_{33}g_{34}u^3S_2 + dg_{11}g_{34}^2u^4S_2 - dg_{11}g_{33}g_{44}u^4S_2 \\
d_2 &= -dg_{11}g_{22}g_{34}u^1S_3 - dg_{22}g_{33}g_{34}u^3S_1 - dg_{22}g_{34}^2u^4S_1 + dg_{22}g_{33}g_{44}u^4S_1 \\
d_3 &= -dg_{11}g_{34}^2u^1S_2 + dg_{22}g_{34}^2u^2S_1 + dg_{22}g_{33}g_{44}u^2S_1 - dg_{11}g_{33}g_{34}u^1S_2
\end{aligned} \tag{3.18}$$

Finally, the last three equations are given by

$$u^4\dot{S}_i + 2\left(\dot{u}_{[4}u_{i]} - u^\alpha u_\rho\Gamma^\rho_{\alpha[4}u_{i]}\right)S_ku^k + 2S_n\Gamma^n_{\alpha[4}u_{i]}u^\alpha = 0 \tag{3.19}$$

which give the derivatives of three spatial components of spin vector ($\dot{S}_i$): $\dot{y}_9$, $\dot{y}_{10}$ and $\dot{y}_{11}$. The full set of the exact MPD equations for the case of a spinning test particle in a Kerr metric under the Pirani condition (2.91) is in appendix [58].

In Appendix A, we write down the full set of MPD equations of motion for a spinning test particle in a Kerr metric. This set is composed by eleven coupled differential equations of first grade.

In the literature, we find that the majority of works are focused by the study of spinless test particles. Therefore, in this part, we work the particular case where the test particle does not have spin and compare our numerical calculations for this case.

First, we have the traditional form of MP equations is [8]

$$\frac{D}{ds}\left(mu^\lambda + u_\mu\frac{DS^{\lambda\mu}}{ds}\right) = -\frac{1}{2}u^\beta S^{\rho\sigma}R^\lambda_{\beta\rho\sigma}. \tag{3.20}$$

We consider the motion of a spinning test particle in equatorial circular orbits ($\theta = \pi/2$) of the rotating source, that is, $a/r \ll 1$ and MG/c^2. For this case we take [58]

$$u^1 = 0, \;\; u^2 = 0, \;\; u^3 = const \neq 0, \;\; u^4 = const \neq 0 \tag{3.21}$$

when the spin is perpendicular to this plane, with

$$S_1 \equiv S_r = 0, \;\; S_2 \equiv S_\theta \neq 0, \;\; S_3 \equiv S_\varphi = 0 \tag{3.22}$$

The equation is given by

$$\begin{aligned} &-y_1^3 y_7^2 - 2\alpha y_7 y_8 + y_8^2 - 3\alpha\varepsilon_0 y_7^2 + 3\varepsilon_0 y_7 y_8 - 3\alpha\varepsilon_0 y_8^2 y_1^{-2} \\ &+3\alpha\varepsilon_0 y_1^2 y_7^4 - \alpha\varepsilon_0 \left(1 - \frac{2}{y_1}\right) y_8^4 y_1^{-3} + \alpha\left(y_1^6 - 3y_1^5\right) y_7^3 y_8 y_1^{-3} + \\ &\alpha\varepsilon_0 \left(3y_1^3 - 11y_1^2\right) y_7^2 y_8^2 y_1^{-3} + \varepsilon_0 \left(-y_1^3 + 3y_1^2\right) y_7 y_8^3 y_1^{-3} = 0 \end{aligned} \tag{3.23}$$

For the case when the particle does not have spin the set of equations (3.20) with the dimensionless quantities y_i (3.1) and (3.2) is given by

$$-y_1^3 y_7^2 - 2\alpha y_7 y_8 + y_8^2 = 0 \tag{3.24}$$

where $\alpha = a/M$.

In addition to Eq. (3.24), we take the condition $u_\mu u^\mu = 1$ and obtain

$$-y_1^2 y_7^2 + 4\alpha \frac{y_7 y_8}{y_1} + \left(1 - \frac{2M}{y_1}\right) y_8^2 = 1. \tag{3.25}$$

We solve the system of equations (3.24) and (3.25) for the case of a circular orbit and obtain the values of $y_7 = Mu^3$ and $y_8 = u^4$.

This system of coupled differential equations of second order is composed of seven equations with seven unknowns and this will be solved via the numerical integration. The system has as output the Cartesian coordinates (x, y, z) which are drawn in 3D. These graphics change according the initial conditions such as the mass M, the radius r, the density of angular momentum a and the four velocity vector (dx^{μ}/ds). The numerical table that comes from this work will be compared with the results given by the Carter´s equations [18] in the next chapter.

3.2 Carter´s equations

In this section, we will study the equations of motion for test particles in a Kerr type space time via Carter´s equations. These equations will be given both for orbits in equatorial planes and spherical orbits, that is, non equatorial planes [60].

3.2.1 Equatorial orbits for spinless test particles

In the equatorial plane and with a constant radius, the Carter´s equations are reduced to

$$\begin{aligned} \Sigma\dot{t} &= a\left(J - aE\right) \\ &\quad + \frac{\left(r^2 + a^2\right)\left[E\left(r^2 + a^2 - aJ\right)\right]}{\Delta}, \end{aligned} \tag{3.26}$$

$$\Sigma\dot{\varphi} = J - aE + \frac{a}{\Delta}\left[E\left(r^2 + a^2\right) - aJ\right], \tag{3.27}$$

where J, E , and Q are constants and

$$\Sigma := r^2 + a^2 \cos^2 \theta, \tag{3.28}$$

$$\Delta := r^2 + a^2 - 2Mr.$$

In the Carter´s equations, the orbital angular frequency es given by

$$\Omega = \frac{d\varphi}{dt} = \frac{\Delta J - \Delta aE + a\left[E\left(r^2 + a^2\right) - aJ\right]}{\Delta a\left(J - aE\right) + \left(r^2 + a^2\right)\left[E\left(r^2 + a^2 - aJ\right)\right]}. \tag{3.29}$$

If we compare this last expression for angular frequency with the expression obtained for the MPD equations we find that for the Carter´s equations the values of the motion constants J, E and M, remain while for the first formulation the result is given by the mass M, and the radius (r) of the orbit.

3.2.2 Equatorial orbits for spinning test particles

In the previous section, we considered the four equations for the motion of particles when they are orbiting in a space time Kerr type (2.106 - 2.109). These equations have four constants of motion: the mass in rest (m), the energy (E), the projection of angular momentum in the rotation axis (J), and the Carter´s constant (Q). When this last constant is equal to zero we guarantee that the motion is restricted to the equatorial plane of the central source, Eq. (2.108). The solution of these equations was given with the help of the numerical integration. Knowing the value of the constants of motion and the initial conditions, it is possible to find the trajectory of a spinning test particle [24]. This property is expressed as

$$p^{\mu}\xi_{\mu} - \frac{1}{2}\xi_{\mu;\nu}S^{\mu\nu} = \text{ constant} \tag{3.30}$$

A Kerr metric admits two Killing vectors $\xi_4{}^i = \delta_4{}^i$ and $\xi_\varphi{}^i = \delta^i_\varphi$, which are own of the stationary nature and axial symmetry. So the two constants of motion with spin are given by

$$\begin{aligned} p_4 + \frac{1}{2} g_{4\mu,\nu} S^{\mu\nu} &= -E \\ p_3 - \frac{1}{2} g_{3\mu,\nu} S^{\mu\nu} &= J \end{aligned}$$

We replace the values of line elements and the system of equations will be give by [24]

$$\begin{aligned} p_4 &= \left[-E + \frac{M\hat{S}}{r^3} (aE - J) \right] \left(1 - \frac{M\hat{S}^2}{r^3} \right)^{-1} \\ p_\varphi &= \left[J + E\hat{S} - \frac{M\hat{S}a}{r^3} (Ea - J) \right] \left(1 - \frac{M\hat{S}^2}{r^3} \right)^{-1} \end{aligned}$$

where $\hat{S} = S/m$.

3.2.3 Spherical orbits for spinless test particles

For the case where the particle orbits in trajectories that are out of equatorial plane, the Carter´s constant Q is different of zero. In this case, it is necessary to calculate the values of Q and J which depend on the values of E, r and a. To find the values (Q and J), the following conditions are imposed [18]

$$\frac{\partial R}{\partial r} = 0, \qquad \frac{\partial^2 R}{\partial r^2} < 0, \tag{3.31}$$

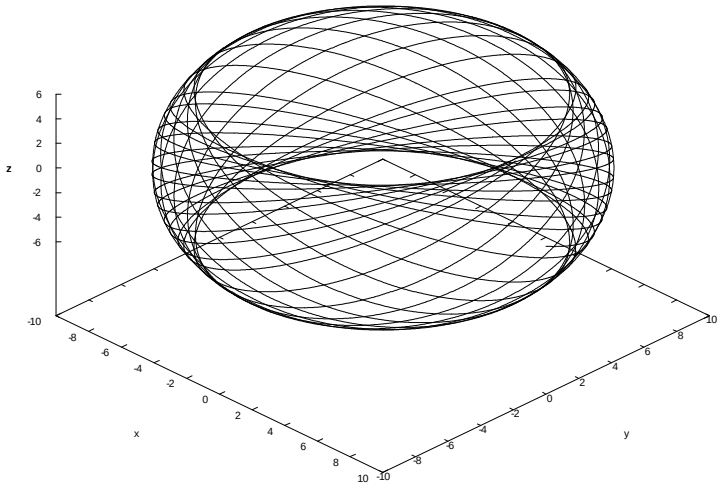

Figure 3.1: Orbit with radius $r = 10$, the constans $Q = 4.224806$ and $J = 2.810974$. Maximum latitude $\theta = 53.9292°$

in the Equation (2.107) from the first integrals of motion. The first condition has relation with the type of orbits, in this case, we call spherical orbits, that is, with constant radius. The second expression has relation with the stability condition of the orbits. The first equation has two signs, that is, this equation gives two simultaneous equations which can be solved for to obtain Q and J in function of E, r and a.

As we wrote before, this system of equations (2.106 - 2.109) can be solved using numerical integration methods [18]. We input the values of E, r and a in the equations (2.107, 2.108 and 2.109) for to find the spatial coordinates of the orbits (Figure 3.1).

In the study of the orbits of test particles in a Kerr metric, there is a class of orbits called spherical. This type of orbits intersects the equatorial plane in a point called node. Since the metric has an angular momentum, the nodes of the spherical orbits are dragged in the same direction of the spin of rotating massive body. When there is a particle orbiting in a nonequatorial orbit, this traces a kind of helix that

ascends until a maximum point of latitude and when reachs it, the particle begins to descends until a minimum point of latitude which is symmetric to the maximum point [18].

The program code given by Kheng *et al.* [18] yields information with respect to the characteristics of the orbits, the maximum value of latitude and the value of movement of node, in the equatorial plane, when the particle pass from a hemisphere to another. To this point is called ascend node. This node is displaced each time that the particle complets an orbit because the particle is submited to a dragging force in the same direction of rotation of the central mass.

3.2.4 Spherical orbits for spinning test particles

When the spinning particle travels in different planes to equatorial plane, symmetries associated with a motion constant do not exist (3.30), therefore the calculation of the equations of motion for spinning test particles in non equatorial planes with the help to Carter´s equations is more complex.

Chapter 4

Gravitomagnetism and spinning test particles

We present experiments which are associated with the study of trajectories of test particles around the rotating massive bodies as is the *Gravity Probe B* experiment. Then, we will study the phenomena with regard to the analogy between the Maxwell equations and the field theory of Einstein which is also called gravitomagnetic effects [62].

4.1 *Gravity Probe B* experiment

Gravity Probe B (GP-B) is an experiment whose objetive is to detect the Lense - Thirring effect when is measured the precession of an orbiting gyroscope. This experiment was thought of fifty years ago, but it was two years ago, before the first experimental results were given to know. Basically it was designed to prove two fundamentals predictions of General Relativity from Einstein. On the one hand, the curvature of spacetime exerts a torque in a gyroscope that orbits around a rotating

mass, in this case the Earth. This preccession is 6.6 arcseconds per year and is called the geodetic effect [28]. The same phenomenon around a mass without rotation is called geodesic effect. This experiment sought to measure the dragging effect of the rotation of the Earth on a gyroscope orbiting around to it. For this case, the measurement is 39 miliarc seconds per year. This phenomenon was predicted by Joser Lense and Hans Thirring in 1918, but it was only in the 60's that George Pugh and Leonard Schiff set out the experiment to measure it with the help of gyroscopes [27].

In the experiment of *Gravity Probe B* (GP-B) four gyroscopes were installated in a satellite which was orbiting to 640 kilometers of the Earth in a polar plane. This satellite was fitted to focus on the far away star "IM Pegasi" and had four drives for to keep the same polar orbit all the time. The four gyroscopes were set out in a line, two of them were turning in a clockwise direction and the other two counter clockwise. The axis of the rotation of each gyroscope was oriented in different directions with the purpose of detecting any movement in any direction. These gyroscopes are totally spheric crystalls and are covered by Niobium a super conductive material. In this way when they turn on, the supercurrents in the Niobium produce a magnetic momentum parallel to the spin axis. So this system is able to detect any change in the orientation of magnetic mometum of a gyroscope and of course the precession in the rotation predicted by the General Relativity [28]. The results are showed in the Figure 4.1.

The relativistic deviation in the direction north - south (Geodetic effect) for the assumption of the General Relativity is 6606,1 miliarc second per year, while for the west-east deviation (Dragging effect) is 39.2 miliarc second per year. According to the average of the four gyroscopes used in *Gravity Probe B* is 6601.8 ± 18.3 miliarc seconds per year for the geodetic effect and 37.2 ± 7.2 miliarc seconds per year for

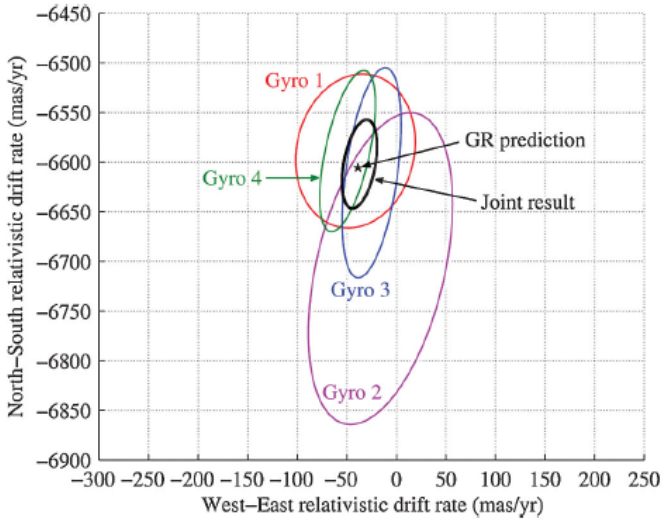

Figure 4.1: Experimental results from *Gravity Probe B* taken from Everitt, C.W. and *et al.* Phys. Rev. Lett. **106**, 221101 (2011).

dragging effect. This experiment is considered high precision and confirms once more the two phenomena predicted by the General Relativity.

The satellite transports the four gyroscopes that are orbiting in a height of 640 km and the rotation axis of gyroscope experiments a dragging of its inertial frame. The reason for the change of the precession is given by the equation

$$\dot{\Omega}_G = \frac{3}{2}\frac{GM}{c^2\mathbf{R}^3}\left(\mathbf{R}\times\mathbf{v}\right) + \frac{GI}{c^2\mathbf{R}^3}\left[\frac{3\mathbf{R}}{\mathbf{R}^2}\left(\omega_e\cdot\mathbf{R}\right) - \omega_e\right] \tag{4.1}$$

where M, I and ω_e are, respectively the mass, the inertial momentum and angular rotation of massive body. The vectors $\mathbf{R}$ and $\mathbf{v}$ are the position and the velocity of the gyroscope relative to the center of the mass of body. The first term is the Sitter precession and is calculated as 6.6 miliarc seconds per year for the gyroscope of GP-B; and the second term, the dragging system of Lense- Thirring of 39 miliarc seconds per year.

4.2 Gravitomagnetic effects

There is a formal analogy between the Coulomb law for the electrostatic and the law of Gravitation of Newton. This analogy describes the newtonian gravitation in terms of a gravitoelectric field [63]. The gravitomagnetic effects concern firstly the electric field. Then, this effect has a relationship with the magnetic field [66]. The gravitomagnetic field is generated by the movement of the matter. In the above section, we studied the experiment of Gravity Probe B (GP-B) which had its as purpose the measurement of the dipolar gravitomagnetic field generated by the Earth with some superconductive gyroscopes on board a satellite that traveled around the Earth [61].

In the second chapter, we linearized the gravitational field equations and found the approximated solution for the Einstein field equation. This set of equations lead to the analogy with Maxwell´s equations [33].

In some cases, when the Einstein equations are perturbed about flat spacetime, they can be written in a form similar to Maxwell´s equations where the Newtonian gravitational field corresponds to the gravito-electric field and mass-currents have an analogy to the electric currents [64]. In addition, since the laws of electromagnetism are well studied, this analogy has proved to be a good source of study to understand the phenomena of gravito-electromagnetism. Now, any theory that combines both the Newtonian gravity and Lorentz invariance must include the study of gravito-magnetism effects which are generated by mass current. One of these cases it is the Lense-Thirring effect in which a rotating mass generates a gravitomagnetic effect, which causes a precession of planetary orbits.

In recents works, there have been possible improvements in the study of the Lense - Thirring precession [65], for instance the experiment to observe the effects of the

gravitomagnetism of the Earth, this is GP-B [27]; the experiment GP-C which reveals the space-time structure and evidences clock effects around a spinning massive body.

In the study of test particles around of rotating massive bodies there exist some phenomena in regard to the gravitomagnetism effects such as the Lense-Thirring effect which describes the precession of the orbital plane when the test particle is orbiting the rotating central source, the Schiff effect which characterizes the spin of the test particle when is orbiting the rotating body and the gravitomagnetic clock effect which describes the delay time for two test particles traveling around a rotating body [53].

There is an analogy between the Lense-Thirring precession and the precession of the angular momentum of a charged particle, orbiting around a magnetic dipole. The gravitomagnetic field produced by a spinning mass, as measured by the congruence of static observers, is similar to the magnetic field produced by a spinning charge [45].

With regard to the delay time, i.e., the gravitomagnetic clock effect which refers to different time for two clocks orbiting a rotating body, on a prograde orbit and on a retrograde orbit. This phenomemum was studied first by Cohen and Mashhoon in 1993. They considered that two clocks on circular equatorial orbits traveling on the same orbit, but in opposite directions have a traveling time difference of:

$$\tau_+ - \tau_- \approx 4\pi \frac{J}{mc^2}. \tag{4.2}$$

4.2.1 Gravitomagnetic coupling between Spin and Angular momentum

In the study that with regards to the rotation of spinning test particles around rotating massive bodies, we find that there is a coupling between the angular momentum of the test particle and the angular momentum of the central mass. In addition, it is possible to clarify this phenomenon via the gravitomagnetic effects.

A spinning particle around a rotating massive body possesses a gravitomagnetic dipole moment which couples to the gravitomagnetic field produced by the rotating mass with an interaction energy analogous to the magnetic interaction

$$H = -m \cdot B \tag{4.3}$$

where m is the magnetic dipole and B the magnetic field. The effects of this coupling have been studied and it wasfound that the paths of circularly polarized photons, in the gravitational field of rotating body, split because of the coupling between the helicity and the angular momentum of the source, much like in a Stern-Gerlach experiment with polarized matter passing through an anisotropic magnetic field [33].

In our study we take the Kerr metric linearized as gravitational field, with the gravitational potentials

$$\Phi \equiv \frac{M}{r}, \qquad \overrightarrow{A} \equiv \frac{\overrightarrow{J} \times \overrightarrow{r}}{r^3}, \qquad \Theta_{ij} \equiv \Phi \delta_{ij}. \tag{4.4}$$

The electromagnetic potentials are

$$\phi \equiv \frac{Q}{r}, \qquad \overrightarrow{A} \equiv \frac{\overrightarrow{\mu_s} \times \overrightarrow{r}}{r^3}. \tag{4.5}$$

In the gravitational case, we are working with linearized theory, so we consider electromagnetic fields weak enough that only their linear contributions are relevant to the dynamics. In the weak field regime, when the particles are at rest, there is a gravitational spin-spin force analogous to the electromagnetic one.

There is an another gravito-electromagnetic analogy, it is the decomposition of the Maxwell tensor $F^{\alpha\beta}$ in electric and magnetic fields and the decomposition of the Riemann tensor (in vacuum) in electric and magnetic tidal tensors [45]. In the equatorial plane of Kerr spacetime the gravito-magnetic tidal tensor vanishes for some velocity field, in analogy with the vanishing of the magnetic field. In other words, for some velocities the magnetic dipole does not precess. First, we take the case electromagnetic as a guide for the gravitational case. The Maxwell tensor splits into the two spatial vectors (3 independent components each)

$$\begin{aligned} E^{\alpha} &\equiv F^{\alpha\beta}u_{\beta} \\ B^{\alpha} &\equiv \star F^{\alpha\beta}u_{\beta} \end{aligned} \tag{4.6}$$

which are the electric and magnetic fields as measured by an observer of four-velocity u^{α}.

The electromagnetic field produced by a spinning charge (magnetic moment $\overrightarrow{\mu}$) is described by the four potential $A^{\alpha} = \left(\phi, \overrightarrow{A}\right)$:

$$\begin{aligned} \phi &= \frac{Q}{r} \\ \overrightarrow{A} &= \frac{1}{c}\frac{\overrightarrow{\mu} \times \overrightarrow{r}}{r^3}. \end{aligned} \tag{4.7}$$

4.2.2 Gravitomagnetic effect in the equatorial plane: Clock effect

In this section we make use of a gravito-electromagnetic analogy between the decomposition of the Maxwell tensor $F^{\alpha\beta}$ in electric and magnetic fields and the decomposition of the Riemann tensor (in vacuum) in electric and magnetic tidal tensors We can compare the scalar invariants of $F^{\alpha\beta}$ and the invariants of $R_{\alpha\beta\gamma\delta}$, and studied in the equatorial plane of Kerr metric that, for some velocities, the gravito-magnetic tidal tensor vanishes [66]. It is analogous to the vanishing magnetic field (not the magnetic tidal tensor). The explanation for this last situation is that a magnetic dipole with those velocities does not precess. For the gravitational case, we investigate if there is a velocity for gyroscopes such that they do not precess relative to the distant stars [67]. The result positive is important in the context of the study of the curvature [26].

First, we have as a guide the electromagnetic system to study the gravitational case. With regard, to the four-vector u^{α}, the Maxwell tensor splits into the two spatial vectors, which are a covariant definition for the electric and magnetic fields:

$$(E^{u})^{\alpha} \equiv F^{\alpha\beta}u_{\beta} \qquad \text{and} \quad (B^{u})^{\alpha} \equiv *F^{\alpha\beta}u_{\beta} \tag{4.8}$$

where the Maxwell tensor $F^{\alpha\beta}$ and its dual $*F^{\alpha\beta}$ are measured by an observer of four-velocity u^{α} as

$$F_{\alpha\beta} = 2u_{[\alpha}\left(E^{u}\right)_{\beta]} + \epsilon_{\alpha\beta\gamma\delta}u^{\delta}\left(B^{u}\right)^{\mu}; \tag{4.9}$$

$$*F_{\alpha\beta} = 2u_{[\alpha}\left(B^{u}\right)_{\beta]} - \epsilon_{\alpha\beta\gamma\sigma}u^{\sigma}\left(E^{u}\right)^{\gamma}. \tag{4.10}$$

Combining $(E^{u})^{\alpha}$ and $(B^{u})^{\alpha}$ one can construct the two second order scalar in-

variants:

$$E^{\alpha}E_{\alpha} - B^{\alpha}B_{\alpha} = -\frac{1}{2}F_{\alpha\beta}F^{\alpha\beta} \tag{4.11}$$

$$E^{\alpha}B_{\alpha} = -\frac{1}{4}F_{\alpha\beta} * F^{\alpha\beta}. \tag{4.12}$$

The physical interpretation for these two scalar invariants is: first, if $E^{\alpha}B_{\alpha} \neq 0$ then the electric E^{α} and magnetic B^{α} fields are both non-vanishing for all observer; second, if $E^{\alpha}E_{\alpha} - B^{\alpha}B_{\alpha} > 0\,(< 0)$ and $E^{\alpha}B_{\alpha} = 0$, there are observers u^{α} for which both the magnetic field $(B^{v})^{\alpha}$ and the electric field $(E^{u})^{\alpha}$ are equal to zero [61].

The components for the magnetic field $(B^{u})^{\alpha} \equiv *F^{\alpha\beta}u_{\beta}$ seen by an arbitrary observer are given by

$$B^{r} = \frac{2\mu_{s}\cos\theta}{r^{3}}u^{t}, \qquad B^{\theta} = \left(\frac{u_{s}u^{t}}{r^{4}} - \frac{u^{\phi}Q}{r^{2}}\right)\sin\theta,$$

$$B^{\phi} = \frac{Qu^{\theta}}{r^{2}\sin\theta}, \qquad B^{t} = \frac{\mu_{s}}{r^{3}}\left(2u^{r}\cos\theta + ru^{\theta}\sin\theta\right)$$

where Q is the static point charge and μ_{s} is the electromagnetic moment.

In the equatorial plane, the condition $B^{r} = 0$ implies $\theta = \pi/2$, the second condition $B^{t} = 0$ implies $u^{\theta} = 0$, and the third condition $B^{\theta} = 0$ implies $u^{\phi}/u^{t} = \mu_{s}/\left(Qr^{2}\right)$. If we assume that the charge and mass are identically distributed in the body, its gyromagnetic ratio is $\mu_{s}/J = Q/2M$, and we conclude that observers with angular velocity

$$v^{\phi} = \frac{u^{\phi}}{u^{t}} = \frac{J}{2Mr^{2}} \equiv v^{\phi}_{(\mathbf{B}=\mathbf{0})}, \tag{4.13}$$

see a vanishing magnetic field in the equatorial plane [61].

Now, we have a test particle which is orbiting in a rotating field. In the previous chapter, we obtained the MPD equations for the cases of test particles with spin and without spin in a rotating field. In this part, we have the set of equations for motion

and study the gravitomagnetic effect when the spinning test particles are orbiting an equatorial plane.

First, we take the traditional form of MP equations whose set of equations is given by [74]

$$\frac{D}{ds}\left(mu^{\lambda}+u_{\mu}\frac{DS^{\lambda\mu}}{ds}\right)=-\frac{1}{2}u^{\pi}S^{\rho\sigma}R^{\lambda}_{\pi\rho\sigma} \tag{4.14}$$

$$\frac{DS^{\mu\nu}}{ds}+u^{\mu}u_{\sigma}\frac{DS^{\nu\sigma}}{ds}-u^{\nu}u_{\sigma}\frac{DS^{\mu\sigma}}{ds}=0 \tag{4.15}$$

where $u^{\lambda}\equiv dx^{\lambda}/ds$ is the four velocity of the particle. In addition, we need a spin supplementary condition (SSC) for fully describing the trajectory of the particle´s center of mass. We have two conditions; the Mathisson-Pirani supplementary condition [41]:

$$S^{\lambda\nu}u_{\nu}=0 \tag{4.16}$$

and the Tulczyjew-Dixon condition [68]:

$$S^{\lambda\nu}P_{\nu}=0 \tag{4.17}$$

where

$$P^{\nu}=mu^{\nu}+u_{\lambda}\frac{DS^{\nu\lambda}}{ds} \tag{4.18}$$

is the four momentum.

We have the equation for the spin evolution under Mathisson-Pirani condition (4.16), simplifies to

$$\frac{DS_{\mu}}{ds}=\epsilon_{\mu\alpha\beta\nu}U^{\nu}u^{\alpha}B^{\beta} \tag{4.19}$$

or, equivalently:

$$\frac{DS_\mu}{ds} = S_\nu a^\nu U_\mu + \epsilon_{\mu\alpha\beta\nu} U^\nu u^\alpha B^\beta \tag{4.20}$$

where $a \equiv DU^\alpha/ds$ denotes the acceleration, and B^β is the magnetic field as measured by the spinning test particle. The first term in (4.20) embodies the Thomas precession; the second term is a torque $\tau = \overrightarrow{\mu} \times \overrightarrow{B}$ causing the Larmor precession of a magnetic dipole under the influence of a magnetic field [45]. In this case, "precession" of the gyroscope is an artifact of the reference frame, with no local physical meaning.

With the goal of calculating the value of the clock effect both for the spinless test particles and for the spinning test particles, we will obtain the set of MPD equations for two cases in equatorial plane from a rotating gravitational field. Then we will solve numerically this set of equations and obtain the cartesian coordinates (x, y, and z) of the trajectories of these test particles when they are traveling in the same direction of the rotating body and in the opposite direction.

Clock effect with spinless test particles

In general, we have a Kerr metric and calculate the equations of motion for spinless test particles with radius constant ($dr/ds = 0$) in the equatorial plane [14]. The equation is given by

$$g_{tt,r}\left(\frac{dt}{d\varphi}\right)^2 + 2g_{t\varphi,r}\left(\frac{dt}{d\varphi}\right) + g_{\varphi\varphi,r} = 0. \tag{4.21}$$

The solutions for this equation (4.21) are

$$\frac{dt}{d\varphi} = a \pm \frac{1}{\omega_K} \tag{4.22}$$

where $\omega_K^2 = M/r^3$ is the keplerian frequency. The equation (4.22) is integrated from 0 until 2π for the co-rotating orbits and from 0 a -2π for counter-rotating orbits for spinless test particles. The integration is given by $t_\pm = T_K \pm 2\pi a$, where $T_K = 2\pi/\omega_K$ is the keplerian period. The gravitomagnetic clock effect is

$$t_+ - t_- = 4\pi a. \tag{4.23}$$

In the particular case of a spinless test particle in a gravitational field, the traditional form of the MPD equations (4.14 and 4.15) is reduced to the equation of geodesics

$$\frac{Du^\lambda}{ds} \equiv \frac{du^\lambda}{ds} + \Gamma^\lambda_{\alpha\beta} u^\alpha \frac{dx^\beta}{ds} = 0. \tag{4.24}$$

The set of equations for spinless particles is given by

$$\dot{u}^3 + \dot{u}^4 + \Gamma^1_{33}\left(u^3\right)^2 + 2\Gamma^1_{34}u^3u^4 + \Gamma^1_{44}\left(u^4\right)^2 + \Gamma^2_{33}\left(u^3\right)^2 + \Gamma^2_{34}u^3u^4 = 0 \tag{4.25}$$

where a dot denotes differentiation with respect to the proper time s. In the other hand, we have the relationship

$$u_\mu u^\mu = 1. \tag{4.26}$$

The second equations is given by

$$u^4 = \left(1 - \frac{2}{r}\right)^{-\frac{1}{2}} \sqrt{1 + r^2\left(u^3\right)^2}. \tag{4.27}$$

With the equations (4.25) and (4.27), we calculate the values of u^3 and u^4.

Clock effect with spinning test particles

Tanaka *et al.* studied the trajectories of spinning test particles in circular orbits for a Kerr metric when the spin value is fixed and orthogonal to equatorial plane [1]. The orbital angular velocity is given by

$$\Omega := \frac{d\varphi}{dt} = \pm \frac{\sqrt{M}}{r^{3/2} \pm a\sqrt{M}} \left[1 - \left(\frac{3S_\perp}{2} \right) \frac{\pm\sqrt{Mr} - a}{r^2 \pm a\sqrt{Mr}} \right] \tag{4.28}$$

where $S_\perp := S^2$.

For the particular case of a spinning test particle with a fixed value, the gravitomagnetic effect is given by [14]

$$t_+ - t_- = 4\pi a - 6\pi S. \tag{4.29}$$

If we compare with the spinless test particles, we found there is an extra element given by the spin of the particle (S). Even, according to this expression (4.29), there would be a special case and is when $a = 3S/2$. In this case, there would not be a shift of time between the particles that travel in the same orbit around of the rotating mass.

Now, we take the MPD equations when the spinning test particles is orbiting in the equatorial plane of a weak Kerr metric at Mathisson-Pirani condition (4.16). In this particular case, we have

$$u^1 = 0, \quad u^2 = 0, \quad u^3 = \text{ constant}, \quad u^4 = \text{ constant}$$

and

$$S^{12} = 0, \quad S^{23} = 0, \quad S^{13} \neq 0.$$

The equations are given by

$$\Gamma^1_{33}\left(u^3\right)^2 + 2\Gamma^1_{34}u^3u^4 + \Gamma^1_{44}\left(u^4\right)^2 + \Gamma^2_{33}\left(u^3\right)^2 = -\frac{2u_4u^3}{\sqrt{-g}}S_2R^1_{313} \tag{4.30}$$

where g is the determinant of the metric tensor. We have the relationship $u_\mu u^\mu = 1$ and write the coordinate u^4 through u^3 as

$$u^4 = \left(1-\frac{2}{r}\right)^{-\frac{1}{2}}\sqrt{1+r^2\left(u^3\right)^2}. \tag{4.31}$$

Inserting u^4 from (4.31) into equation (4.30) we obtain the expression for u^3:

$$\begin{aligned} &\Gamma^1_{33}\left(u^3\right)^2 + 2\Gamma^1_{34}u^3\left(1-\frac{2}{r}\right)^{-\frac{1}{2}}\sqrt{1+r^2\left(u^3\right)^2} + \\ &\Gamma^1_{44}\left(1-\frac{2}{r}\right)^{-1}\left(1+r^2\left(u^3\right)^2\right) + \Gamma^2_{33}\left(u^3\right)^2 \\ = \quad &-\frac{2\left(1-\frac{2}{r}\right)^{-\frac{1}{2}}\sqrt{1+r^2\left(u^3\right)^2}u^3}{\sqrt{-g}}S_2R^1_{313} \end{aligned} \tag{4.32}$$

We yield the exact numerical solution for the case when two spinning test particles describe circular orbits in the equatorial plane and travel in opposite sense. This gravitomagnetic phenomenum is called clock effect. We take the MPD equations (4.14) and (4.15) for a Kerr metric and the Mathisson-Pirani spin supplementary condition $S^{\lambda\nu}u_\nu = 0$. For this, we write the code in C++ and obtain the initial values by the four velocity (dx^μ/ds) and the spatial values for the spin vector (S_i). The code is in Appendix A.

For cheking our results, we review the papers with regarts to gravitomagnetic clock effect [21] and compare their numerial results with ours. There is a phenomenon called the gravitomagnetic clock effect which consists of a difference in the time it takes for two test particles to travel around a rotating massive body in opposite

directions [2]. This difference is given by $t_+ - t_- = 4\pi a/c$, where $a = J/Mc$ is the angular density of the central mass. Tartaglia has studied the geometrical aspects of this phenomenon [69], [70] and Faruque yields the equation of the gravitomagnetic clock effect with spin as

$$t_+ - t_- = 4\pi a - 6\pi S_0, \tag{4.33}$$

where S_0 is the magnitude of the spin.

In true units this relation is given by

$$t_+ - t_- = \frac{4\pi J_M}{Mc^2} - \frac{6\pi J}{mc^2}, \tag{4.34}$$

where the first relation of the right could be used to measure J/M directly for an astronomical body; in the case of the Earth $t_+ - t_- \simeq 10^{-7}\,\mathrm{s}$, while for the Sun $t_+ - t_- \simeq 10^{-5}\,\mathrm{s}$ [80].

4.3 Michelson - Morley type experiments

Historically the Michelson-Morley experiment was done to measure the effects of ether on the traveling time of a light beam . In the experiment, a beam of light is sent from a source s, is split in two perpendicular paths, which are recombined the beams, to observe the resulting interference fringes in the process final [71]. A calculation shows that the motion of the earth with a speed v should cause the light traveling along a path parallel to the direction to take longer than light traveling along a path perpendicular to the direction of motion, the difference in travel time being

$$\Delta t = \frac{L}{c}\frac{v^2}{c^2} \tag{4.35}$$

to second order in v/c, where L is the lenght of the interferometer arms. If the interferometer rotates ninety degrees, Michelson expected to shift of interference fringes equal to 0.4 fringe. What he measured was at most 0.01 fringe shift. This is generally interpreted as a null result [72]. In this experiment there are two implict assumptions: first, that, there exists an absolute reference frame in which light travels at a constant speed $c = 3.00 \times 10^8\,\mathrm{m/s}$ relative to this reference frame, and second, that, the geometry of the interferometer is not changed by its motion.

The first explanation for the null result in the experiment was proposed by Fitzgerald and Lorentz. They abandoned the second assumption. They consi-dered that if the arm of the interferometer in the direction parallel to the directions of motion shrank by a factor of $\sqrt{1 - v^2/c^2}$, the expected fringe shift would be exactly canceled, resulting in the observed null result. This explanation did not gain general acceptance.

The second explanation was presented by Einstein who chose a philosophical explanation to abandon the first assumption, assuming the non-existence of an absolute reference frame. Even though it is an important point, the special theory of relativity considers that the non-existence of an absolute reference frame, does not prove this non-existence, only the impossibility of detecting it from an inertial reference frame

In this section, we study the interferometer where the source of the field is rotating, thus the situation in principle changes. In other words, there is a tiny anisotropy, depending on the angular momentum of the source. In other works, we studied the influence of the angular momentum density on a Michelson-Morley type experiment [73]. In this case, we shall include not only the angular momentum of the central source, but also the spin for describing the trajectory of the test particle when it travels in each arm of the interfometer. Numerical calculations will show that the effects are quite small in any case, however the results will give values comparable

with those expected and planned to measured with big interferometric detectors like LIGO and VIRGO .

In general the Michelson-Morley type experiments are located in two dimensions which consist in two perpendicular arms. There is an observer in the inertial frame who measures the time of beams of light from the source until the beams are collected in a pattern of interference after colliding with a screen at the end of each arm. In our case, we have a challenge because we are studying trajectories of spinning test particles in three dimensions, while, in many papers, the authors describe these orbits only in the equatorial plane. Since we only have an observer that measures the time of the two spining particles travelling around a massive rotating body when they do a lap, we will just take the projection of the trajectories in a spatial plane of two dimensions (Cartesian coordinates: x, y) after an orbit, that is, when $x = x_0$(radius) $y = 0$; then we will measure the difference of distance and finally will calculate the delay time for these two trajectories that travel in opposite directions.

Chapter 5

Conclusions, remarks and future works

At the start of this research we took the works on General Relativity with regards to the dynamics of extended bodies orbiting around massive rotating bodies. The first step was to study the equations of motion for test particles, both in equatorial planes and in non equatorial planes, given by Carter and the study of Mathisson-Papapetrou-Dixon equations for test particles with spin and non spin.

With help of the numerical calculation, we found the trajectories of spinning test particles around a rotating massive body. The type of trajectory is given by the features of the gravitational field and for the relationship between the angular momentum of massive body and the spin of the test particle. First of all, we found that the central mass exerts a drag on inertial systems. This phenomenon is compared with a magnetic field via an analogy called gravitomagnetic effect [26]. When we calculate the coordinate time of a lap both in the direction of the angular momentum of the central source and in the opposite direction, we found a delay time with regards to a fixed observer with respect to the fixed starts. This phenomenon is called clock

effect [2]. Also, we concluded that the difference of time decreases with the spin value, even though this delay time is higher when the spinning test particle does not have restrictions in its spin direction. We proved numerically that the clock effect decreases with the spin and is neglected for a particular value. This phenomenon is not only related to the dragging from the central mass but also to the coupling of the angular momentum of the rotating field with the intrinsic angular momentum of the test particle.

One of the goals of this thesis is to research the influence of both the angular momentum of the central mass and the spin value of the test particle in Michelson-Morley type experiments. Tartaglia and Ruggiero, in one of their papers, set up a interferometer which its horizontal arm coincident with the equatorial plane of the rotating massive body and its vertical arm with one of the polar planes [73]. If two spinning test particles get out from the same point and each one travels respectivally for each arm a determined distance; then, these spinning test particles come back to the initial point, found different situations. The spinning test particle takes a one-way and one-time return traveling for the horizontal arm of the interferometer. A time for the trip when the test particle goes in the same direction of rotation of the central mass and an other time when the test particle comes back for the same arm but in opposite direction to the rotation of the rotating field. Then, we take the round trip time for the spinning test particle when it is traveling along the vertical arm of the interferometer. As the trip along the horizontal arm, the spinning test particle experiments a delay time due to the dragging of the rotating massive body. This delay time is not only caused by the dragging of the central mass, but also by the coupling between the angular momentum of the central source and the spin of the test particle [14].

Regarding to the gravitomagnetic effect, this phenomenon is not only influenced

by the angular momentum of the central source, but also for the angular momentum of the test particle. There is a relationship between the gravitational field and the angular momentum of the particle. The numerical calculations that we obtained in this research show clearly that central mass in rotating exerts a drag on the inertial frames around to it, but on the other hand, the direction of spin axis of the test particle experiences a tiny deviation when the latter orbits around to the central source [70]. In this way, it is proved the need to establish a coupling between the particle spin and the rotating gravitational field, therefore it is necessary to explain these phenomena with the field theory more than distant forces to the Newtonian mode.

Phenomena such as the gravitomagnetics effects are conjugated the large scales, because massive bodies at very large angular velocities, but the features of these phenomena arise on very small scales. The study of these situations will provide elements to address physical phenomena such as the gravitational waves which are produced by masses of astronomical order, but they are too small to be detected by the traditional instruments. This is still an open question for the astrophysics, the way in which these waves can be detected, and characterized [34].

There is a mutual relationship between the description of the movement of spinning test particles with the description of rotating space-time by which that particle is displaced, so that when studying the characteristics of motion is given in the same time the features of space-time. Checking one more time the link the displacement and the gravitational field where is traveling the test particle.

Most of the calculations are located in very high values for the central mass just as for the angular momentum; however, there is the limit for weak gravitational fields as the Earth and for unrelativistic velocities. This in order to describe phenomena close to the earth´s surface and objects orbiting around it such satellites [29]. The

description of these phenomena contributes to the advancement of technologies such as the global position system or comunication satellites.

Phenomena such as the Lense Thirring effect, where the mass current carry out a drag of the inertial systems in the equatorial plane or the precession of gyroscope spin, called Schiff effect have been studied in the equatorial plane. With this research, this can be extended to trajectories of spinning test particles in non equatorial planes where phenomena are characterized in another way [45].

To set up Michelson-Morley type experiments that take the totality of an orbit around from the central source and with a scales of larger time, perhaps a year, where the particles orbit such as the case of *Gravity Probe B*, which took more of a year to register the shift both of the Lense Thirring effect and the geodetic effect for the space time curvature [28]. Even the construction of this experiment is complex, and it is possible to use geostationary satellites for proving the effects both from mass currents generated by the rotation of central mass, and the spin effects of the particle when this later is moving in contrary sense [48].

5.1 Numerical comparison of the two methods

Each one of the formulations studied in last chapter (MPD equations and Carter´s equations), has a set of coupled differential equations. It is impossible solving the system of analytical way, only for some exceptional cases [74]. Since this limitation, we proceed to solve these systems with help of numerical integration. For each one of the methods, we take the cartesian coordinates (x, y, z) of the test spinning particle in a Kerr space time. As in the last section, we will take two cases: spinless and spinning test particles [59].

The aim of this section is to restore the numerical results that are presented

in the literature [18], for this case of spinless test particles both in the equatorial plane and in the spherical orbits. We will compare our results with the numerical integration with the results given of Carter´s equations for to validate the method of MPD equations. After we will take this data and will compare both for the case without spin and with spin under the MPD equations.

5.1.1 Equatorial orbits for spinless test particles

We take two set of parameters in order to attach the initial conditions of the trajectories: First set belongs to central mass and the second set has relation with the test particle. With regards to central mass, one has the density of angular momentum (a) which relates the angular momentum to the unit of mass. The maximum value allowed is $a = M$, where M is the mass of the central mass. Further, in this section we take the spinless test particles, i.e., the particles which do not have spin.

A property of the Kerr metric (2.3) is when the denominator of coefficient for the dr^2 component tends to zero, this term goes to infinity. This is the radius that defines the horizon of event of rotating massive body and is given by

$$r_h = M + \sqrt{M^2 - a^2}. \tag{5.1}$$

In this case $M = a$ the horizon of event is in $r = M$. For values of $a > M$ there are not real radii in which the horizon of event exists.

The mass of a massive body is defined as M and in many of the calculations that we will do, we will give it the value of one. In this decision there is not lost of generalitiy because the other quantities related with M can be rescaled by reason of M.

Basically we will take three parameters for describing the motion of a spinless

particle. First the angular momentum of the particle per unity of mass (J) in the ϕ direction of the central source due to Lense - Thirring effect. Second, the energy per unit of mass of the particle (E). This parameter corresponds to the total energy of the particle. A stationary particle in the infinity with respect to the rotating massive body will have $E = 1$ (in geometrized units). For coupled orbits $|E| < 1$ y $E < 0$ correspond to the values of energy of orbits inside of the ergosphere. In this tesis, we will work positive energies, that is $0 < E < 1$. Finally, the third parameter is the Carter´s constant (Q) which was given by Carter ([6]). This conserved quantity of a particle in free fall around to a rotating mass affects the latitudinal movement and is related with the orbital angular momentum of the particle in the θ direction. From the Equation (2.108) we can study, in the equatorial plane, the relation between Q and the motion in θ

$$r^2\dot{\theta}^2 = Q. \tag{5.2}$$

From the equation (2.108) we can deduce that for bounded orbits ($E \leq 1$), Q must always be positive. In addition, for that the orbit will be stable we impose the condition that the radius should be constant for an allow radius, that is

$$\dot{r} = \frac{dr}{d\tau} = 0 \Longrightarrow R = 0 \tag{5.3}$$

where R is from the Equation (2.107). In this case there is no radial velocity. The second condition for stable orbits is

$$\frac{\partial R}{\partial r} = 0 \tag{5.4}$$

which ensures that there is not radial acceleration for given radius. This last equation

gives two simultaneous equations which can be solved to obtain Q and L as functions of E, r and a. The equations are

$$Q = \frac{r^2}{a^2\left(1-r\right)^2}[1-E^2]. \tag{5.5}$$

5.1.2 Equatorial orbits for spinning test particles

We calculate the Cartesian coordinates (x, y, z) for the case when the spinning test particle is orbiting in an equatorial plane around on a rotating massive body. The code in C++ (see Appendix A) needs the initial condition both for the four position vector (x^μ) and the four velocity vector (dx^μ/ds). The particle is traveling in the plane when $\theta = \pi/2$ and the polar component is equal zero $(d\theta/ds = 0)$.

We use as step size $h = 2^{-25}$. The numerical calculation uses integral powers of 2. The aim of this choice is to avoid rounding off error in the step size. In this numerical work the double precision minimizes rounding errors.

The choice of the fourth-order Runge Kutta method is to provide a suitable balance between error and computational time [75]. The average of computational time is around four weeks, even in some cases the CPU took twelve weeks. On the other hand, a typical calculation involves 500 million iterations, and needs a lot of memory. There were cases where the program yielded more of one billion lines.

In general, we obtained three types of graphs: the first one draws the trajectory of spinning test particle orbiting around a rotating massive body. The orbit is a circle of radius $r = 10$ (geometrized units). As we will see later, we obtain the trajectories when the particle travels in the same sense of the central body and the contrary direction.

The second graph is the magnitude of the spin vector versus coordinate time (t). We work the case when the spin is orthogonal to the equatorial plane $(S_2 \neq 0)$. For

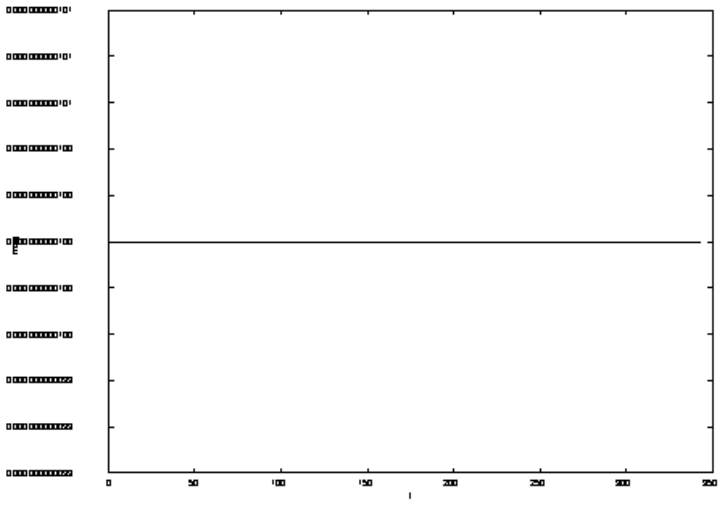

Figure 5.1: The magnitude of the spin when the spinning particle is orthogonal to the equatorial plane ($S_2 \neq 0$)

this case, the magnitude of spin is constant (Figure **??**).

The third graph describes the orbital motion and the helical motion, therefore the trajectory is almost a sinusoidal curve around on a circle (Figure 5.3). This shape is given by the supplementary spin condition which is the Mathisson-Pirani condition

$$S^{\mu\nu}u_{\mu} = 0. \tag{5.6}$$

The paper by Costa *et al.* explains the reason why this motion is helical and is considered a physical situation [42]. Given the MP condition the center of mass is shiftted from its proper center and the body experiments a "hidden momentum" which moves the spinning particle more to one side. Therefore the motion of the particle is helical.

5.1.3 Numerical calculate of the MPD equations

We calculate numerically the MPD equations as presented by Plyastsko *et al.* [15] for the particular case of a spinning test particle in the field of rotating massive body

for a constant radius. We take the set of the eleven equations (3.5 - 3.19) and deduce the eleven differential equations of the dimensionless quantities y_i (Appendix B). We write the code in C++ language and with help of the four order Runge-Kutta method [75], we yield the trajectory of a spinning test particle in Cartesian coordinates (x, y, z). We use the signature $(-, -, -, +)$, the Boyer - Lindquist coordinates (r, θ, ϕ, t), Latin indices run $1, 2, 3$ and Greek indices $1, 2, 3, 4$. Geometrized units $(c = 1, G = 1)$

We introduce in the code the initial values and obtain four tables of data. First, the Cartesian coordinates (x, y, z) of the trajectory of a spinning test particle orbiting to a massive rotating body in the equatorial. Second table, the program will output the spatial coordinates of the 3-vector of spin (S_1, S_2, S_3). Third table, the magnitude of 3-vector of spin versus the coordinate time (t). Fourth table, the graph both on the orbital motion and the nutation of the spinning particle.

Particular case: $r = 10$

In order to check out our results, we take the particular case $(r = 10)$ given by Kheng *et al.* in their project "Massive Particle Orbits Around Kerr black Holes" (Unpublished, 2007) [18]. The radius $r = 10$ is in geometrized units. Given this radius, we calculate the E-range whose allowed values are $0.95191 \leq E_{r=10} \leq 0.96292$. With the energy value (0.9525), we find the constants: Carter´s constant (Q) and the angular momentum (J), with the conditions (3.31). The constants of motion are given: energy (E), Carter´s constant (Q), z-component of angular momentum (J_z), mass (M) and angular momentum density of central body (a). Given these values, we calculate the initial value of four vector velocity $(dx_0^\mu/ds = dr_0/ds, d\theta_0/ds, d\phi_0/ds, dt_0/ds)$ with the set of Carter´s equations (2.106 - 2.109). Finally, we take the set of MPD equations given by Plyatsko *et al.* (3.1 - 3.19) and yield the phase space for the

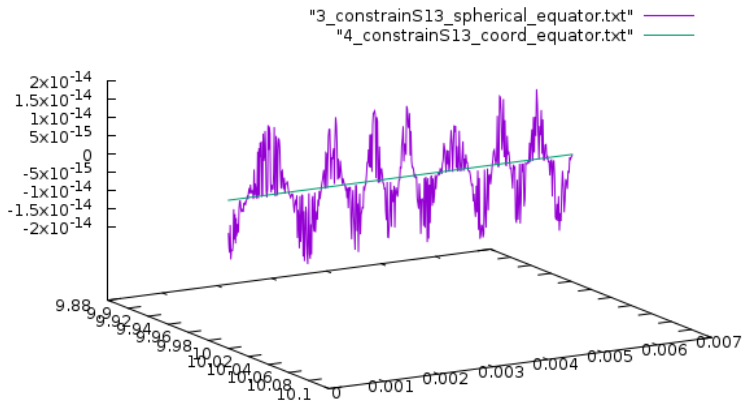

Figure 5.2: The nutation of a spinning test particle with Pirani condition

spatial components of three vector of spin (S_1, S_2, S_3).

Graphs for this case

The program code (Appendix A) in C++ language outputs three graphs in particular: the Cartesian coordinates of the trajectory of a spinning test particle orbiting around a massive rotating body, the magnitude of the spin and the motion of the spinning particle both orbital and the nutation.

We obtain different kinds of graphs, the first graph describes in Cartesian coordinates the gyro axis z of the spinning test particle which is perpendicular to equatorial plane initially. Then, the top of axis describes a tiny circumference in the plane $z-y$ (Figure 5.2). The radius of this circumference is 1×10^{-10}.

We do a second graph with the help of these two graphs and obtain a spherical cycloide. That is, a curve generated by a curve rolling on another curve [76]. According with the Pirani´s spin condition, we should obtain a helicoidal movement [77] inside a world tube.

If we draw at the same time the orbital motion and the spin motion, we obtain an

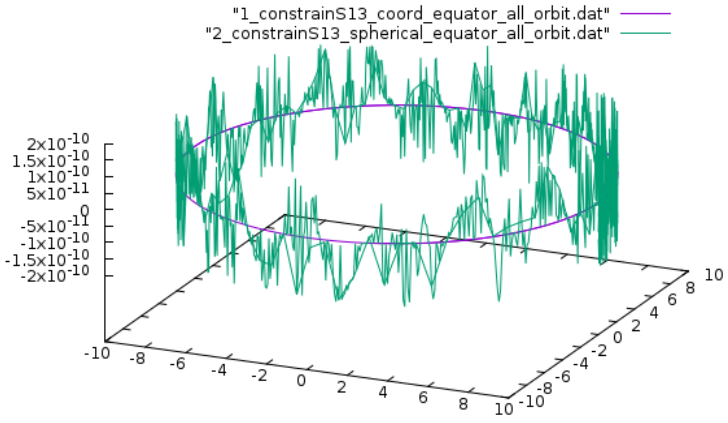

Figure 5.3: The trajectory of a spinning test particle with the spin supplementary condition of Pirani has a helical motion

ascending and descending movement within an enveloping sinusoidal wave (Figure 5.3). This movement is called "bobbing" [78]. Moreover, this ascendent and descendent movement is due to the supplementary spin condition that we take which is the MP condition ($S^{\mu\nu}u_\nu = 0$), where u_ν is the center of mass four velocity. In this situation, the center of mass is measured in its proper frame (that is, the frame is at rest). This phenomenon is due the shiftting of the center of mass, and in addition, the momentum of the particle not being parallel to its four-velocity in general. There is a “hidden momentum" that produces this nutation. In an analogy with the electric (E) and magnetic (B) fields, there would be $E \times B$ drift, that is, the motion is described by helical motions [79]. Costa *et al.* describe this physical situation, due to the supplementary condition [61].

Numerical results for the spinning test particles

When we calculate numerically the MPD equations, we take two cases for the spin of the particle. The first one, the spin of the test particle is orthogonal to the equatorial plane. In this case, the spatial components r and ϕ are constrained in the time. The

test particle is defined as S_2. For the second case, the spatial components of the particle (S_1, S_2, S_3) can revolve around on its gyro axis.

For these two cases, we take the same initial conditions both for the position vector and for the four velocity vector in the particular case when $r = 10$.

The period of time for the spinning test particle when it travels orthogonal to the equatorial plane $(S_2 \neq 0)$ both for the prograde orbit and for the retrograde orbit is given in geometrized units as (time has the dimension of length)

$$\begin{aligned} t_+ &= 334.07729152971453\,\mathrm{m} \\ t_- &= 326.53881036659527\,\mathrm{m} \\ \Delta t &= 7.5384116316618189\,\mathrm{m} \end{aligned} \tag{5.7}$$

According with the numerical results, the spinning test particle when it travels in the opposite sense to the motion of the source central, takes longer to reach its starting point than the test particle that is traveling in the same sense (5.7). In other words, there is clear influence of the angular momentum of the rotating massive body with respect to the motion of the spinning test particle. This phenomenon is produced by the dragging of the inertial systems and is called Lense - Thirring effect. In addition, there exists an analogy between the Maxwell equations and the linearized field equations of Einstein that was studied above.

In the case of the spinning test particle in which is not restricted in the spin orientation $(S_1 \neq 0, S_2 \neq 0, S_3 \neq 0)$, the period of time both for the prograde orbit

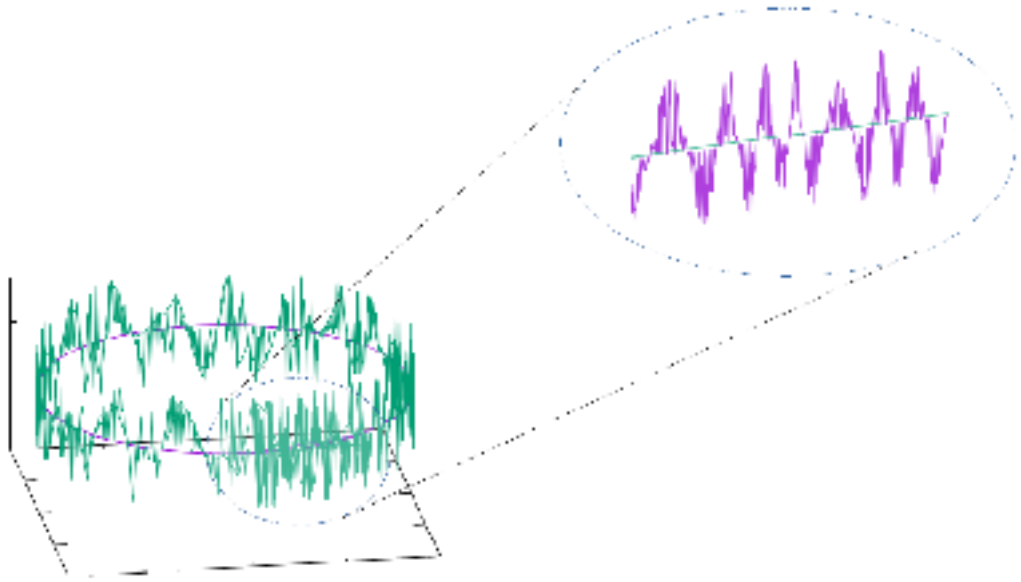

Figure 5.4: Detail of the bobbing of the spinning test particle in the circular orbit

and for the retrograde orbit is given in geometrized units as

$$\begin{aligned} t_{+} &= 514.73954619635052\,\mathrm{m} \\ t_{-} &= 512.89836830460433\,\mathrm{m} \\ \Delta t &= 1.8411778917461561\,\mathrm{m} \end{aligned} \tag{5.8}$$

As in the case of the orthogonal spin, there is a delay time when the spinning test particle travels in the same sense as the rotation of source central or the opposite sense. Moreover of the Lense - Thirring effect, the difference of time between the orthogonal spinning test particle (5.7) is longer than the difference for the spinning test particle that rotates freely in its three axes.

When we compare the period of time for a spinning test particle that does not have restrictions in the spin orientation (5.8), with the period for a spinning test particle that is orthogonal to equatorial plane (5.7) we find that the former takes more time to complete a lap than the test particle that is perpendicular to the

equatorial plane. According to these results, the test particle with more degrees of freedom in the spin needs more time in to arrive at the point of departure. Therefore, there is a influence both on the angular momentum of the central source and on the rotating gravitational field in the trajectory of the test particle [80].

5.1.4 Numerical calculate of Carter´s equations

As fruit of a project in National University of Singapore, Kheng *et al.* [18] considered a particle orbiting around a rotating massive body. They, with help of Carter´s equations studied the equations of motion for spherical orbits, that is, with radius constant and in non equatorial planes. The first step for obtaining the allowed ranges of E is to find the boundary lines of these range. Therefore, the conditions from the equation (2.107) are imposed

$$\frac{\partial R}{\partial r} = 0, \qquad \frac{\partial^2 R}{\partial r^2} < 0 \tag{5.9}$$

Given these conditions, the $E-$range table for differents radius is calculated [18]. For our study, we take as radius of comparation $r = 10$ in geometrized units. For the latter radius the allowed values of E are $0.95191 \leq E_{r=10} \leq 0.96292$.

With the first equation of the two above conditions (5.9), it is possible to obtain two simultaneously which can be solved to yield Q and J as functions of E, r and a. The equations for obtaining Q and J are given by

$$
\begin{aligned}
Q_1 &= \frac{r^2}{a^2\left(1-r\right)^2}\left[\begin{array}{c}\left(1-E^2\right)r^4+\left(4E^2-5\right)r^3+\left(8-5E^2\right)r^2\\ +\left(2aE^2-a^2-4\right)r+a^2\\ +2E\Delta\sqrt{r\left[1+r\left(E^2-1\right)\right]}\end{array}\right]\\
J_1 &= \frac{1}{a\left(r-1\right)}\left[Er^2-a^2E-\Delta\sqrt{r\left[1+r\left(E^2-1\right)\right]}\right] \qquad (5.10)
\end{aligned}
$$

where $\Delta = r^2 - 2mr + a^2$.

The next step is to replace the values of E and r in the last equations and obtaining Q and J for a given radius. Then, to replace the values of r, E, Q and J in the Carter´s equations so we obtain the components of the four velocity vector (dx/ds). With these inputs, the code will output the spatial coordinates (x, y, z) of the orbits.

Numerical results for the spinless test particles

In this section, we calculate the numerical results from the spinless test particles. In the code, we take the step as 2^{-22} and the value of the revolution equal to 1.01 both in the retrograde motion and prograde motion. The program yiels the following values in geometrized units:

$$
\begin{aligned}
t_+ &= 216.08928266085720\,\mathrm{m}\\
t_- &= 203.522912056498\,\mathrm{m}\\
\Delta t &= 12.5663706043592\,\mathrm{m} \qquad (5.11)
\end{aligned}
$$

This result (5.11) is the delay time for the case when two spinless test particle are orbiting around a rotating massive body in the same orbit, but in opposite sense.

5.1.5 Comparing the numerical results for the two methods

In the case of the MPD equations, we calculate numerically the time for spinning test particles when they orbit around to a rotating massive body and find that the spinning test particle that travels in the opposite direction to the rotation of the central mass takes more time to complete a lap. For the case of the spinless test particles, the phenomenon is the same. The spinless test particle that orbits in a contrary direction takes more time in to complete a lap (5.11) than the particle that travels in the same direction with the rotation of the central mass. On the other hand, the difference in time for a spinless test particle (5.11) is longer than the difference both for a spinning test particle which is orbiting perpendicular to the equatorial plane (5.7) and for the spinning test particles that do not have restrictions in the spin orientation (5.8). Even the difference of time decreases when the degrees of freedom increase [81]. The difference of time reduces from 11.114332 m for the spinless test particles to 1.8411778917 m for the spinning test particles.

We evaluate the delay time for the two methods in non-geometrized units, that is, the factors of G and c must be reinserted. In this case, the conversion factor relative to geometrized units for a quantity with dimension of time is c for the difference in

time in the two cases that we had studied is given by

$$\begin{aligned}
&\text{For spinless test particles } (S_i = 0) \\
\Delta t &= 4.191724408539 \times 10^{-8}\,\mathrm{s} \\
&\text{For orthogonal spinning test particle } (S_1 = 0, S_2 \neq 0, S_3 = 0) \\
\Delta t &= 2.521207903565826 \times 10^{-8}\,\mathrm{s} \\
&\text{For spinning test particle without restriction } (S_i \neq 0) \\
\Delta t &= 0.615778559112427 \times 10^{-8}\,\mathrm{s}
\end{aligned} \tag{5.12}$$

According to the analytical solution, the equation (4.33) predicts that the clock effect is reduced by the spin value of the test particle [14]. If we take the difference between the clock effect for spinless test particles and the clock effect when the test particles have spin, we obtain

$$\Delta t = 4\pi a - 6\pi S. \tag{5.13}$$

Now we take the numerical solution for the two cases and obtain

$$\begin{aligned}
\Delta t_{spinless} - \Delta t_{spin_S2} &= 1.6705165049732 \times 10^{-8}\,\mathrm{s} \\
\Delta t_{spinless} - \Delta t_{spin_S123} &= 3.5759458494266 \times 10^{-8}\,\mathrm{s}.
\end{aligned} \tag{5.14}$$

According to these results, the delay time increases when the spinning test particle does not have restrictions in the spin orientation.

5.2 Effects by spin

In this section, we study the trajectories of spinning test particles in the equatorial plane. As we have mentioned before, in addition to MPD equations (4.14) and (4.15), it is necessary to add a spin suplementary condition for choosing the particle´s center of mass. We have the Mathisson-Pinari condition

$$S^{\lambda\nu}u_{\nu} = 0. \tag{5.15}$$

By this condition the components S^{i4} can be expressed through S^{ik}:

$$S^{i4} = \frac{u_k}{u_4}S^{ki}. \tag{5.16}$$

Sometimes, it is more convenient to express the spin tensor in spatial components by the relationship

$$S_i = \frac{1}{u_4}\sqrt{-g}\varepsilon_{ikl}S^{kl} \tag{5.17}$$

where ε_{ikl} is the spatial Lévi-Cività symbol.

For the equatorial case, according the motion of the spin the particle has a precession which is described by the projection of the head of the particle in three dimensions. This precession is caused by the relationship between the curvature of space time with angular momentum of the particle (Figure 5.4). For the numerical calculation, we take two cases: first, when the components radial (S_1) and azimuthal (S_3) are constrained, that is, we take the axis of spin perpendicular to equatorial plane, and second, there is no restriction on the components of gyro by spin. For the first case, the projection of spin in 3D describes a tiny tilted circular orbit. For the other case, the projection makes up a bunch of trajectories whose are embedded in a sphere. This is because in general the value of spin is not constant [38], [82].

The other set of graphs describe the magnitude of the spin versus proper time. When the components radial (S_1) and azimuth (S_3) of the spin or the components radial (S_1) and polar (S_2) are constrained simultaneously the magnitude is constant (Figure **??**).

Above, we study the case where the two spinning test particles travel in opposite direction and in the same orbit. Also, the spin axis is parallel to the central axis of the rotating massive body. In this part, we take the case where the spin axis is antiparallel to the axis of the central mass. In this case, the trajectory of the spinning test particle has a helical movement too. However, if we compare these two trajectories, we found a phase difference and a different interaction between spin - spin [78].

5.2.1 Futures works

Like almost all the research, this thesis gave us many answers about the motion of spinning test particles in a Kerr metric in the equatorial plane, but also, it presents many questions for future work, among others, the movement of test particles in a non-equatorial plane. In the near future, we will be studying the gravitomagnetism effects in planes out of the equator and the relationship between in the angular momentum of the central mass and the particle spin when the particle is rotating in a rotating field. In this section, we will describe the basics elements for the study of gravitomagnetic phenomena in non-equatorial planes.

Tidal Tensors in Gravitational and Electromagnetic fields

In the second chapter, we studied that the motion of a spinless test particle is described by a geodesic. Then, we studied the spinning test particles and found that the trajectories of theses particles deviate from the way of the geodesics. This devia-

tion is described by the geodesic deviation equation. We take the geodesic deviation equation for studying the tidal forces in gravity whose are given by

$$\frac{D^2\delta x^\alpha}{ds^2} = -R^\alpha_{.\mu\beta\sigma}U^\mu U^\sigma \delta x^\beta \tag{5.18}$$

this equation describes the relative acceleration between two neighbouring particles with the same four-velocity U^α. There is a ratio between gravitational and inertial mass, but the ratio between electrical charge and inertial mass does not exist, that is, there is no electromagnetic counterpart of the equivalence principle. In electrodynamic, the worldline deviation equation is

$$\frac{D^2\delta x^a}{ds^2} = \frac{q}{m}F^\alpha_{.\mu;\beta}U^\mu \delta x^\beta, \tag{5.19}$$

where $F_{\alpha\beta}$ is the Maxwell tensor. Thereby, there is a physical analogy between the two tensors:

$$\mathrm{E}_{\alpha\beta} \equiv R_{\alpha\mu\beta\sigma}U^\mu U^\sigma \longleftrightarrow E_{\alpha\beta} \equiv F_{\alpha\mu;\beta}U^\mu \tag{5.20}$$

where $E_{\alpha\beta}$ is the covariant derivative of the electric field $E^\alpha = F^{\alpha\beta}U_\beta$ seen by the observer of four velocity field U^α. This is called electric tidal tensor and $\mathrm{E}_{\alpha\beta}$ is known as electric part of the Riemann tensor or the electric gravitational tidal tensor. From the electric tidal tensor is defined the magnetic tidal tensor as

$$B_{\alpha\beta} \equiv \star F_{\alpha\mu;\beta}U^\mu = \frac{1}{2}\varepsilon^{\gamma\lambda}_{\ldots\alpha\beta}F_{\gamma\lambda;\beta}U^\mu \tag{5.21}$$

where $\star$ means the Hodge dual and $\varepsilon^{\gamma\lambda}_{\ldots\alpha\beta}$ is the Levi-Civita tensor. The tidal effects given by magnetic field $B^\alpha = \star F^{\alpha\beta}U_\beta$ are measured by the tensor $B_{\alpha\beta}$. There is an

analogy with the magnetic part of the Riemman tensor

$$\mathrm{H}_{\alpha\beta} \equiv \star R_{\alpha\mu\beta\sigma}U^{\mu}U^{\sigma} = \frac{1}{2}\varepsilon^{\gamma\lambda}_{\ldots\alpha\beta}R_{\gamma\lambda\beta\sigma}U^{\mu}U^{\sigma}. \tag{5.22}$$

Therefore, there is a physical gravitational analogue of $B_{\alpha\beta}$:

$$B_{\alpha\beta} \longleftrightarrow \mathrm{H}_{\alpha\beta}. \tag{5.23}$$

On the other hand, the Maxwell equations are tidal equations and are defined by electromagnetic tidal tensor as:

$$\begin{aligned} E^{\alpha}_{.\alpha} &= 4\pi\rho_c \\ E_{[\alpha\beta]} &= \frac{1}{2}F_{\alpha\beta;\gamma}U^{\gamma} \\ B^{\alpha}_{.\alpha} &= 0 \\ B_{[\alpha\beta]} &= \frac{1}{2}\star F_{\alpha\beta;\gamma}U^{\gamma} - 2\pi\varepsilon_{\alpha\beta\sigma\gamma}j^{\sigma}U^{\gamma} \end{aligned} \tag{5.24}$$

where j^{α} and $\rho_c = -j^{\alpha}U_{\alpha}$ are respectively, the current four-velocity and the charge density as measured by the observer of four-velocity U^{α}. The tensors are expressed by

$$\begin{aligned} F_{\alpha\beta;\gamma}U^{\gamma} &= 2U_{[\alpha}E_{\beta]\gamma}U^{\gamma} + \varepsilon_{\alpha\beta\mu\sigma}U^{\sigma}B^{\mu\gamma}U_{\gamma} \\ \star F_{\alpha\beta;\gamma}U^{\gamma} &= 2U_{[\alpha}B_{\beta]\gamma}U^{\gamma} + \varepsilon_{\alpha\beta\mu\sigma}U^{\sigma}E^{\mu\gamma}U_{\gamma} \end{aligned} \tag{5.25}$$

Maxwell´s field equations in vacuum are

$$F^{\mu}_{\ .\nu;\mu} = 0, \qquad F_{[\mu\nu;\alpha]} = 0 \tag{5.26}$$

We split the Maxwell tensor into the two spation vector fields for observers with four-velocity field U^α as

$$E^\alpha = F^\alpha_\beta U^\beta, \qquad B^\alpha = \star F^\alpha_{.\beta} U^\beta \tag{5.27}$$

Now, let be E_α and B_α two tensorial quantities which are U^α independent, and are given by

$$E^\alpha E_\alpha - B^\alpha B_\alpha = -\frac{F_{\alpha\beta}F^{\alpha\beta}}{2}, \qquad E^\alpha B_\alpha = -\frac{F_{\alpha\beta} \star F^{\alpha\beta}}{4}, \tag{5.28}$$

these are the two independent relativistic invariants in four spacetime dimensions [62].

Spinning charge and spinning mass

We have a sphere of charge q, mass m, rotating with constant angular momentum $J\mathrm{e}_z$ and the contibutions of electric monopole and magnetic dipole, therewith the potential is given by

$$A = -\frac{q}{r}dt + \frac{\mu \sin^2\theta}{r}d\phi \tag{5.29}$$

where $\mu = Jq/2m$ is the magnetic dipole moment of the rotating sphere. This element will be important when we define the motion of the spininng test particle [62].

The electric and magnetic tidal tensors are symmetric for the static observer with 4-velocity $U^\mu = \delta^\mu_0$ as

$$\begin{aligned} E_{\alpha\beta}dx^\alpha dx^\beta &= -\frac{2q}{r^3}dr^2 + \frac{q}{r}d\Omega \\ B_{\alpha\beta}dx^\alpha dx^\beta &= \frac{3\mu}{r^2}\left(-\frac{2\cos\theta}{r^2}dr^2 + \cos\theta d\Omega - \frac{2\sin\theta}{r}drd\theta\right). \end{aligned} \tag{5.30}$$

Trajectories in non-equatorial planes

One of the works that we will do is the study of trajectories of spinning test particles when these particles are traveling in non-equatorial planes and orbiting a Kerr metric.

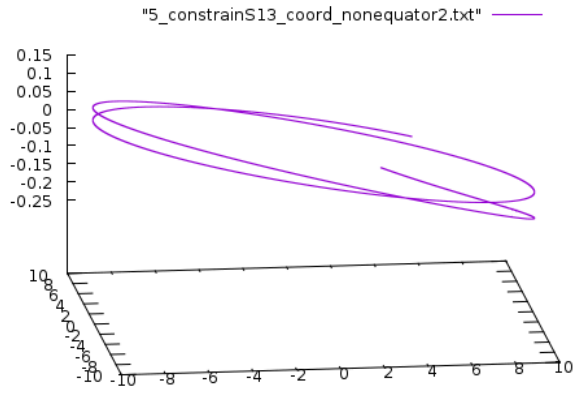

Figure 5.5: The trayectory of a spinning test particles in non-equatorial planes

The code that we worked for the spinning test particles was for the case of a spining test particles orbiting an equatorial plane, now we write the code for the case where the test particle is on the non-equatorial plane (Figure 5.5)

Chapter 6

Appendix A

Program code

```
#include <cstdio>
#include <cstdlib>
#include <cmath>
#include <iostream>
#include <fstream>
using namespace std;
const int N = 12; // Number of equations + 1.
The first one is a dummy
/* Variables */
const double E1 = 0.951906373;
const double y_1 = 1*pow(10,1); /* starting value of r */
const double a = 1;
const double M = 1;
const double y_2 = 1.57079632679;
const double revol = 1.1; /* number of revolutions to run */
```

```
const double stepsize = 10; /* 2^-n */
const double Q = /*(pow(y_1,2)/(pow(a,2)*pow((M-y_1),2)))*
((1-pow(E1,2))*pow(y_1,4)+(4*M*pow(E1,2)-5*M)*pow(y_1,3)+
(8-5*pow(E1,2))*pow(M,2)*pow(y_1,2)+
(2*a*pow(E1,2)-pow(a,2)-4*pow(M,2))*M*y_1+
pow(a,2)*pow(M,2)+2*M*E1*(pow(y_1,2)-(2*M*y_1)+
pow(a,2))*sqrt(y_1*(M-y_1+y_1*pow(E1,2))));
const double J1 = /*(1/(a*(y_1-M)))*(M*E1*pow(y_1,2)-
pow(a,2)*M*E1-(pow(y_1,2)-2*M*y_1+
pow(a,2))*sqrt(y_1*(M-y_1+y_1*pow(E1,2))));
const double y_3 = 0.;
const double y_4 = 0.;
const double y_5 = sqrt(abs(pow((E1*(pow(y_1,2)+pow(a,2))-
a*pow(J1,2)),2)-(pow(y_1,2)-M*y_1+pow(a,2))*(pow(y_1,2)+
Q+pow((J1-a*E1),2))))/(pow(y_1,2)+pow(a,2)*pow(cos(y_2),2));
const double y_6 = sqrt(Q-pow(cos(y_2),2)*(pow(a,2)*
(1-pow(E1,2))+pow(J1,2)/pow(sin(y_2),2)))/(pow(y_1,2)+
pow(a,2)*pow(cos(y_2),2));
const double y_7 = ((J1/pow(sin(y_2),2))-a*E1+(a*(E1*
(pow(y_1,2)+pow(a,2))-a*pow(J1,2))/(pow(y_1,2)-2*M*y_1+
pow(a,2))))/(pow(y_1,2)+pow(a,2)*pow(cos(y_2),2));
const double y_8 = (a*(J1-a*E1*pow(sin(y_2),2))+
(pow(y_1,2)+pow(a,2)/(pow(y_1,2)-2*M*y_1+pow(a,2)))*
(E1*(pow(y_1,2)+pow(a,2))-
a*pow(J1,2)))/(pow(y_1,2)+pow(a,2)*pow(cos(y_2),2));
const double y_9 = pow(10,-10);
```

```
const double y_10 = 157;
const double y_11 = pow(10,-10);
double EPS; /* step size */
const double alpha = (a/M);
void rk4_vector(double t, double h, double y[]);
// Runge-Kutta of four order
double f_dot(const double t, const double y[], const int idx);
int main (void)
{
int i, sgn_y1, sgn_y2, sgn_y1_set = 0., sgn_y2_set = 0.;
double y[N] = {0};
double REVOL;
double c1, c2, c3, Q1, Q2, Q3, Q4, A, C, p, p1, p2, p3, p4,
E1, J1, D, d1, d2, d3;
ofstream foutvariables("constrainS13_variables_equator_minus.txt");
ofstream fout("constrainS13_coord_equator_cycloid_plus.txt");
ofstream foutspin("constrainS13_mov_spin_equator_cycloid_plus.txt");
ofstream foutspinmagplus("constrainS13_mag_spin_equator_cycloid_plus.txt");
ofstream foutcycloid("constrainS13_equator_spherical_cycloid_plus.txt");
/* Evaluating EPS, REVOL and REPT_FREQ */
EPS = pow(2, -stepsize);
REVOL = revol*2*M_PI;
/* specify initial values */
y[1] = y_1;
y[2] = M_PI/2;
y[3] = 0.;
```

```
y[4] = 0.;
y[5] = y_5;
y[6] = y_6;
y[7] = y_7;
y[8] = y_8;
y[9] = y_9;
y[10] = y_10;
y[11] = y_11;
printf("%f %f %f %f %f %f %f %f %f %f %f\n",y[1], y[2], y[3], y[4],
y[5], y[6], y[7], y[8],y[9],y[10],y[11]);
foutvariables<<y[1] << "\t" << y[2] << "\t" << y[3] << "\t" << y[4] <<
"\t" << y[5] << "\t"<< y[6] << "\t"<< y[7] << "\t" << y[8] << "\t"
<< y[9] << "\t" << y[10] << "\t" << y[11] << "\t" << endl;
fout<<y[1]*sin(y[2])*cos(y[3]) << "\t" << y[1]*sin(y[2])*sin(y[3]) << "\t"
<< y[1]*cos(y[2]) << "\t" << endl;
foutspin<<y[9]*sin(y[10])*cos(y[11]) << "\t" << y[9]*sin(y[10])*sin(y[11])
<< "\t"<< y[9]*cos(y[10]) << "\t" << endl;
foutspinmagplus<< y[4]<< "\t" <<sqrt(pow(y[9]*sin(y[10])*cos(y[11]),2)+
pow(y[9]*sin(y[10])*sin(y[11]),2) +
pow(y[9]*cos(y[10]),2)) << endl;
foutcycloid<<(cos(y[3]))*(y[1]-
(cos(pow(tan((sqrt((pow(y[9]*sin(y[10])*cos(y[11]),2))+
(pow(y[9]*sin(y[10]*sin(y[11])),2))))/(y[9]*cos(y[10]))),-1)))*
(sqrt(pow(y[9]*sin(y[10])*cos(y[11]),2)+
pow(y[9]*sin(y[10])*sin(y[11]),2) +pow(y[9]*cos(y[10]),2))-
(sqrt(pow(y[9]*sin(y[10])*cos(y[11]),2)+
```

```
pow(y[9]*sin(y[10])*sin(y[11]),2)+pow(y[9]*cos(y[10]),2)))*
sin((y[1]*y[3])/(sqrt(pow(y[9]*sin(y[10])*cos(y[11]),2)+
pow(y[9]*sin(y[10])*sin(y[11]),2) + pow(y[9]*cos(y[10]),2))))))-
(sqrt(pow(y[9]*sin(y[10])*cos(y[11]),2)+
pow(y[9]*sin(y[10])*sin(y[11]),2) +
pow(y[9]*cos(y[10]),2)))*(sin(y[3]))*
(cos(((y[1]*y[3])/(sqrt(pow(y[9]*sin(y[10])*cos(y[11]),2)+
pow(y[9]*sin(y[10])*sin(y[11]),2) +
pow(y[9]*cos(y[10]),2)))))) << "\t" <<
(sin(y[3]))*(y[1]-(cos(pow(tan((sqrt((pow(y[9]*sin(y[10])*cos(y[11]),2))+
(pow(y[9]*sin(y[10]*sin(y[11])),2))))/(y[9]*cos(y[10]))),-1)))*
(sqrt(pow(y[9]*sin(y[10])*cos(y[11]),2)+ pow(y[9]*sin(y[10])*sin(y[11]),2)
+pow(y[9]*cos(y[10]),2))-(sqrt(pow(y[9]*sin(y[10])*cos(y[11]),2)+
pow(y[9]*sin(y[10])*sin(y[11]),2) +
pow(y[9]*cos(y[10]),2)))*sin((y[1]*y[3])/(sqrt(pow(y[9]*sin(y[10])*cos(y[11]),2)+
pow(y[9]*sin(y[10])*sin(y[11]),2) + pow(y[9]*cos(y[10]),2))))))+
(sqrt(pow(y[9]*sin(y[10])*cos(y[11]),2)+ pow(y[9]*sin(y[10])*sin(y[11]),2)
+pow(y[9]*cos(y[10]),2)))*(cos(y[3]))*
(cos(((y[1]*y[3])/(sqrt(pow(y[9]*sin(y[10])*cos(y[11]),2)+
pow(y[9]*sin(y[10])*sin(y[11]),2) + pow(y[9]*cos(y[10]),2))))))
<< "\t" <<(sin(pow(tan((sqrt((pow(y[9]*sin(y[10])*cos(y[11]),2))+
(pow(y[9]*sin(y[10]*sin(y[11])),2))))/(y[9]*cos(y[10]))),-1)))*
((sqrt(pow(y[9]*sin(y[10])*cos(y[11]),2)+ pow(y[9]*sin(y[10])*sin(y[11]),2)
+pow(y[9]*cos(y[10]),2))-(sqrt(pow(y[9]*sin(y[10])*cos(y[11]),2)+
pow(y[9]*sin(y[10])*sin(y[11]),2) +
pow(y[9]*cos(y[10]),2)))*sin((y[1]*y[3])/(sqrt(pow(y[9]*sin(y[10])*cos(y[11]),2)+
```

```
pow(y[9]*sin(y[10])*sin(y[11]),2) + pow(y[9]*cos(y[10]),2))))))
<< "\t" << endl;
for (i = 1; fabs(y[3])< REVOL; i++)
{
// runge kutta step
rk4_vector(i, EPS, y);
foutvariables<<y[1] << "\t" << y[2] << "\t" << y[3] << "\t"
<< y[4] << "\t" << y[5] << "\t" << y[6]<< "\t"<< y[7] << "\t" << y[8]
<< "\t" << y[9] << "\t" << y[10] << "\t" << y[11] << "\t" << endl;
fout<<y[1]*sin(y[2])*cos(y[3]) << "\t" << y[1]*sin(y[2])*sin(y[3])
<< "\t" << y[1]*cos(y[2]) << "\t" << endl;
foutspin<<y[9]*sin(y[10])*cos(y[11]) << "\t" << y[9]*sin(y[10])*sin(y[11])
<< "\t"<< y[9]*cos(y[10]) << "\t" << endl;
foutspinmagplus<< y[4]<< "\t"<<sqrt(pow(y[9]*sin(y[10])*cos(y[11]),2)+
pow(y[9]*sin(y[10])*sin(y[11]),2) +
pow(y[9]*cos(y[10]),2)) << endl;
foutcycloid<<(cos(y[3]))*(y[1]-(cos(pow(tan((sqrt((pow(y[9]*sin(y[10])*cos(y[11]),2))+
(pow(y[9]*sin(y[10]*sin(y[11])),2))))/(y[9]*cos(y[10]))),-1)))*
(sqrt(pow(y[9]*sin(y[10])*cos(y[11]),2)+ pow(y[9]*sin(y[10])*sin(y[11]),2) +
pow(y[9]*cos(y[10]),2))-(sqrt(pow(y[9]*sin(y[10])*cos(y[11]),2)+
pow(y[9]*sin(y[10])*sin(y[11]),2) +
pow(y[9]*cos(y[10]),2)))*sin((y[1]*y[3])/(sqrt(pow(y[9]*sin(y[10])*cos(y[11]),2)+
pow(y[9]*sin(y[10])*sin(y[11]),2) + pow(y[9]*cos(y[10]),2))))))-
(sqrt(pow(y[9]*sin(y[10])*cos(y[11]),2)+
pow(y[9]*sin(y[10])*sin(y[11]),2) + pow(y[9]*cos(y[10]),2)))*(sin(y[3]))*
(cos(((y[1]*y[3])/(sqrt(pow(y[9]*sin(y[10])*cos(y[11]),2)+
```

```
pow(y[9]*sin(y[10])*sin(y[11]),2) + pow(y[9]*cos(y[10]),2))))))
<<"\t"<<(sin(y[3]))*(y[1]-(cos(pow(tan((sqrt((pow(y[9]*sin(y[10])*cos(y[11]),2))
+(pow(y[9]*sin(y[10]*sin(y[11])),2)))))/(y[9]*cos(y[10]))),-1)))*
(sqrt(pow(y[9]*sin(y[10])*cos(y[11]),2)+ pow(y[9]*sin(y[10])*sin(y[11]),2)
+pow(y[9]*cos(y[10]),2))-(sqrt(pow(y[9]*sin(y[10])*cos(y[11]),2)+
pow(y[9]*sin(y[10])*sin(y[11]),2) +
pow(y[9]*cos(y[10]),2)))*sin((y[1]*y[3])/(sqrt(pow(y[9]*sin(y[10])*cos(y[11]),2)+
pow(y[9]*sin(y[10])*sin(y[11]),2) + pow(y[9]*cos(y[10]),2))))))+
(sqrt(pow(y[9]*sin(y[10])*cos(y[11]),2) + pow(y[9]*sin(y[10])*sin(y[11]),2)
+ pow(y[9]*cos(y[10]),2)))*(cos(y[3]))*(cos(((y[1]*y[3])/
(sqrt(pow(y[9]*sin(y[10])*cos(y[11]),2)+
pow(y[9]*sin(y[10])*sin(y[11]),2) +
pow(y[9]*cos(y[10]),2)))))) << "\t" <<
(sin(pow(tan((sqrt((pow(y[9]*sin(y[10])*cos(y[11]),2))+
(pow(y[9]*sin(y[10]*sin(y[11])),2)))))/(y[9]*cos(y[10]))),-1)))*
((sqrt(pow(y[9]*sin(y[10])*cos(y[11]),2)+ pow(y[9]*sin(y[10])*sin(y[11]),2) +
pow(y[9]*cos(y[10]),2))-(sqrt(pow(y[9]*sin(y[10])*cos(y[11]),2)+
pow(y[9]*sin(y[10])*sin(y[11]),2) +
pow(y[9]*cos(y[10]),2)))*
sin((y[1]*y[3])/(sqrt(pow(y[9]*sin(y[10])*cos(y[11]),2)+
pow(y[9]*sin(y[10])*sin(y[11]),2) +
pow(y[9]*cos(y[10]),2)))))) << "\t" << endl;
}
}
void rk4_vector(double t, double h, double y[]) //
Runge-Kutta method of four order
```

```
{
double k1[N], k2[N], k3[N], k4[N];
double ytmp[N];
int ii;
// k1
for (ii = 0; ii < N; ++ii) {
k1[ii] = h*f_dot(t, y, ii);
}
for (ii = 0; ii < N; ++ii) {
ytmp[ii] = y[ii] + k1[ii]/2;
}
// k2
for (ii = 0; ii < N; ++ii) {
k2[ii] = h*f_dot(t + h/2, ytmp, ii);
}
for (ii = 0; ii < N; ++ii) {
ytmp[ii] = y[ii] + k2[ii]/2;
}
// k3
for (ii = 0; ii < N; ++ii) {
k3[ii] = h*f_dot(t + h/2, ytmp, ii);
}
for (ii = 0; ii < N; ++ii) {
ytmp[ii] = y[ii] + k3[ii];
}
//k4
```

```
for (ii = 0; ii < N; ++ii) {
k4[ii] = h*f_dot(t + h, ytmp, ii);
}
// update
for (ii = 0; ii < N; ++ii) {
y[ii] = y[ii] + (1.0/6.0)*(k1[ii] + 2*k2[ii] + 2*k3[ii] + k4[ii]);
}
}
double c1, c2, c3, Q1, Q2, Q3, Q4, A, C,
p, p1, p2, p3, p4, D, d1, d2, d3;
double f_dot(const double t, const double y[], const int idx)
{
// check correct indexes in [1, 11]
printf("%f %f %f %f %f %f %f %f %f %f %f\n",y[1], y[2], y[3], y[4],
y[5], y[6], y[7], y[8],y[9],y[10],y[11]);
if ( idx < 0 || idx >= N)
{
std::cerr << "ERROR: Calling f_dot with erroneous index =
" << idx << endl;
exit(1);
}
double c1, c2, c3, c4, d1, d2, d3, d4, p, p1, p2, p3, p4;
double z, q, psi, eta, chi, Xi, alpha, beta, Delta;
double D, C, Q1, Q2, Q3, Q4, A;
z = pow(y[1],2) + pow(alpha,2)*pow(cos(y[2]),2);
q = y[1]*(y[1] - 2) + pow(alpha,2);
```

```
psi = pow(y[1],2) - pow(alpha,2)*pow(cos(y[2]),2);
eta = 3*pow(y[1],2) - pow(alpha,2)*pow(cos(y[2]),2);
chi = (pow(y[1],2) + pow(alpha,2));
Xi = pow(y[1],2) - 3*pow(alpha,2)*pow(cos(y[2]),2);
p1 = -z*y[5]*pow(q,-1);
p2 = -z*(y[6]);
p3 = (2*alpha*y[1]*y[8]*pow(sin(y[2]),2) -
y[7]*(z*(pow(y[1],2) + pow(alpha,2)) +
2*pow(alpha,2)*y[1]*pow(sin(y[2]),2))*pow(sin(y[2]),2))*pow(z,-1);
p4 = (2*alpha*y[1]*y[7]*pow(sin(y[2]),2) +
y[8]*(z - 2*y[1]))*pow(z,-1);
c1 = y[7]*y[10]*sin(y[2]) - (z - 2*y[1])*y[6]*y[11]*
pow(q,-1)*pow(sin(y[2]),-1);
c2 = y[5]*y[11]*(z-2*y[1])*pow(q,-1)*pow(sin(y[2]),-1)-
y[7]*y[9]*(q*sin(y[2]));
c3 = (y[6]*y[9]*q-y[5]*y[10])*sin(y[2]);
d1 = -(2*alpha*pow(q,-1)*y[1]*y[6]*y[11] + y[8]*y[10])*sin(y[2]);
d2 = (2*alpha*pow(q,-1)*y[1]*y[5]*y[11]+q*y[8]*y[9])*sin(y[2]);
d3 = (y[5]*y[10]-q*y[6]*y[9])*sin(y[2]);
p = 2*alpha*y[1]*y[7]*pow(sin(y[2]),2) + (z - 2*y[1])*y[8];
Q1 = (y[1]*q-z*(y[1]-1))*pow(y[5],2)*pow(z,-1)*pow(q,-1)-
q*y[1]*pow(y[6],2)*pow(z,-1)- q*(y[1]*pow(z,2)-
pow(alpha,2)*psi*pow(sin(y[2]),2))*
pow(y[7],2)*pow(z,-3)*pow(sin(y[2]),2)+
q*psi*pow(y[8],2)*pow(z,-3)-
pow(alpha,2)*y[5]*y[6]*pow(z,-1)*sin(2*y[2])-
```

```
2*alpha*q*psi*y[7]*y[8]*pow(z,-3)*pow(sin(y[2]),2);
Q2 = (-0.5*pow(alpha,2))*pow(z,-1)*pow(y[6],2)*sin(2*y[2])+
0.5*pow(alpha,2)*pow(y[5],2)*pow(z,-1)*pow(q,-1)*sin(2*y[2])-
0.5*pow(y[7],2)*(pow(z,2)*(pow(y[1],2) + pow(alpha,2)) +
2*pow(alpha,2)*y[1]*((pow(y[1],2) + pow(alpha,2)) + z)*
pow(sin(y[2]),2))*pow(z,-3)*sin(2*y[2])
-pow(alpha,2)*pow(z,-3)*y[1]*pow(y[8],2)*sin(2*y[2])+
2*y[1]*y[5]*y[6]*pow(z,-1) +
2*alpha*y[1]*y[7]*y[8]*(pow(y[1],2) + pow(alpha,2))*pow(z,-3)*sin(2*y[2]);
Q3 = 2*y[5]*y[7]*(y[1]*z*(z-2*y[1])-pow(alpha,2)*psi*
pow(sin(y[2]),2))*pow(z,-2)*pow(q,-1)+
2*alpha*y[5]*y[8]*psi*pow(z,-2)*pow(q,-1)+2*y[6]*y[7]*(pow(z,2) +
2*pow(alpha,2)*y[1]*pow(sin(y[2]),2))*
pow(z,-2)*pow(tan(y[2]),-1) -
4*alpha*y[1]*y[6]*y[8]*pow(z,-2)*pow(tan(y[2]),-1);
Q4 = -2*alpha*y[5]*y[7]*(2*y[1]*y[1]*z+psi*(pow(y[1],2) +
pow(alpha,2)))*pow(z,-2)*pow(q,-1)*pow(sin(y[2]),2)+
2*y[5]*y[8]*psi*(pow(y[1],2) + pow(alpha,2))*pow(z,-2)*pow(q,-1)+
2*pow(alpha,3)*y[1]*pow(z,-2)*y[6]*y[7]*
pow(sin(y[2]),2)*sin(2*y[2]) -
2*pow(alpha,2)*y[1]*pow(z,-2)*y[6]*y[8]*sin(2*y[2]);
C = -(1 - 2*y[1]*pow(z,-1))*y[8] -
2*alpha*y[1]*y[7]*pow(z,-1)*pow(sin(y[2]),2) +
2*pow(alpha,2)*q*pow(z,-3)*y[1]*y[7]*y[9] -
2*alpha*q*y[1]*y[8]*y[9]*
pow(z,-3)*cos(y[2])
```

```
+ (pow(y[1],2) + pow(alpha,2))*psi*y[7]*y[10]*pow(z,-3)*sin(y[2]) -
alpha*pow(z,-3)*y[8]*y[10]*psi*sin(y[2])-
2*pow(alpha,2)*y[1]*y[5]*y[11]*pow(q,-1)*pow(z,-2)*cos(y[2])-
y[6]*y[11]*psi*pow(z,-2)*pow(sin(y[2]),-1);
D = -2*pow(alpha,3)*y[1]*pow(z,-3)*y[7]*y[9]*pow(sin(y[2]),4)*cos(y[2])+
q*(pow(z,2) + 2*pow(alpha,2)*y[1]*pow(sin(y[2]),2))*
y[8]*y[9]*pow(z,-3)*cos(y[2])
- alpha*y[7]*y[10]*((pow(y[1],2) + pow(alpha,2))*psi +
2*pow(y[1],2)*z)*pow(z,-3)*pow(sin(y[2]),3)-
y[8]*y[10]*(y[1]*z*(z -2*y[1])-
pow(alpha,2)*psi*pow(sin(y[2]),2))*pow(z,-3)*sin(y[2])
+2*alpha*y[1]*y[5]*y[11]*(pow(y[1],2) +
pow(alpha,2))*pow(q,-1)*pow(z,-2)*cos(y[2])+
alpha*psi*y[6]*y[11]*pow(z,-2)*sin(y[2]) +
pow(p,-1)*(2*alpha*y[1]*pow(y[7],2)*
(z*(pow(y[1],2) +pow(alpha,2))* +
2*pow(alpha,2)*y[1]*pow(sin(y[2]),2))*pow(z,-1)*pow(sin(y[2]),2)
+q*z*y[7]*y[8]*(1-8*pow(alpha,2)*pow(y[1],2)*pow(q,-1)*
pow(z,-2)*pow(sin(y[2]),2)) -
2*alpha*y[1]*(z - 2*y[1])*pow(z,-1)*pow(y[8],2))*pow(sin(y[2]),2);
A = -2*alpha*y[5]*y[6]*y[9]*y[10]*eta*pow(z,-3)*cos(y[2])-
2*alpha*y[5]*y[7]*y[9]*y[11]*eta*pow(z,-4)*((pow(y[1],2) + pow(alpha,2))*+
2*pow(alpha,2)*pow(sin(y[2]),2))*cos(y[2])
-6*alpha*y[1]*y[6]*y[7]*y[9]*y[11]*q*Xi*pow(z,-4)*sin(y[2]) +
6*y[1]*y[6]*y[8]*y[9]*y[11]*q*Xi*pow(z,-4)*pow(sin(y[2]),-1)
+6*alpha*y[1]*pow(y[7],2)*y[9]*y[10]*q*Xi*(pow(y[1],2) +
```

```
pow(alpha,2))*pow(z,-5)*pow(sin(y[2]),3) -
6*y[1]*y[7]*y[8]*y[9]*y[10]*q*Xi*pow(z,-5)*
((pow(y[1],2) + pow(alpha,2))* +
pow(alpha,2)*pow(sin(y[2]),2))*sin(y[2])
+6*alpha*y[1]*pow(y[8],2)*y[9]*y[10]*q*Xi*pow(z,-5)*sin(y[2])+
2*alpha*y[6]*y[7]*y[10]*y[11]*eta*pow(z,-4)*(2*(pow(y[1],2) +
pow(alpha,2))* + pow(alpha,2)*pow(sin(y[2]),2))*cos(y[2])-
6*alpha*y[1]*y[5]*y[10]*y[11]*Xi*(pow(y[1],2) +
pow(alpha,2))*pow(q,-1)*pow(z,-4)*sin(y[2])+
6*pow(alpha,2)*y[1]*y[5]*y[8]*y[10]*y[11]*Xi*pow(q,-1)*pow(z,-4)*sin(y[2])
+alpha*pow(y[6],2)*pow(y[9],2)*q*eta*pow(z,-3)*cos(y[2]) +
alpha*pow(y[7],2)*pow(y[9],2)*eta*q*(pow((pow(y[1],2) +
pow(alpha,2)),2) +
2*q*pow(alpha,2)*pow(sin(y[2]),2))*pow(z,-5)*pow(sin(y[2]),2)*cos(y[2])
- 2*pow(alpha,2)*pow(z,-5)*y[7]*y[8]*pow(y[9],2)*
eta*q*(3*(pow(y[1],2) +
pow(alpha,2)) -4*y[1])*pow(sin(y[2]),2)*cos(y[2])
+ alpha*eta*q*(2*q +pow(alpha,2)*pow(sin(y[2]),2))*pow(z,-5)*pow(y[8],2)*
pow(y[9],2)*cos(y[2])+ alpha*eta*pow(y[5],2)*pow(y[10],2)*
pow(q,-1)*pow(z,-3)*cos(y[2])
- alpha*eta*(2*pow((pow(y[1],2) + pow(alpha,2)),2) +
pow(alpha,2)*q*pow(sin(y[2]),2))*pow(y[7],2)*pow(y[10],2)*
pow(z,-5)*pow(sin(y[2]),2)*cos(y[2])
- alpha*eta*(q +2*pow(alpha,2)*pow(sin(y[2]),2))*pow(y[8],2)*
pow(y[10],2)*pow(z,-5)*cos(y[2]) +
2*pow(alpha,2)*pow(z,-5)*eta*(3*(pow(y[1],2) + pow(alpha,2)) -
```

```
2*y[1])*y[7]*y[8]*pow(y[10],2)*pow(sin(y[2]),2)*cos(y[2])
+ alpha*eta*(q+2*pow(alpha,2)*pow(sin(y[2]),2))*pow(y[5],2)*
pow(y[11],2)*pow(q,-2)*pow(z,-3)*
pow(sin(y[2]),-2)*cos(y[2])-alpha*eta*(2*q+pow(alpha,2)*pow(sin(y[2]),2))*
pow(y[6],2)*pow(y[11],2)*pow(q,-1)*pow(z,-3)*pow(sin(y[2]),-2)*cos(y[2])+
6*alpha*Xi*y[1]*y[5]*y[6]*pow(y[11],2)*pow(q,-1)*
pow(z,-3)*pow(sin(y[2]),-1)
- 4*pow(alpha,3)*pow(y[1],2)*eta*pow(y[7],2)*
pow(y[11],2)*pow(q,-1)*
pow(z,-5)*pow(sin(y[2]),2)*cos(y[2]);
beta = y[5]*y[9]+y[6]*y[10]+y[7]*y[11];
// return appropriate derivate according to indexes
if (idx == 1) {
return 0.;
}
else if (idx == 2) {
return 0.;
}
else if (idx == 3) {
return y[7];
}
else if (idx == 4) {
return y[8];
}
else if (idx == 5) {
return 0.;
```

```
}
else if (idx == 6) {
return -(((-C - E1 + c1*Q1 + c2*Q2 + c3*Q3)*y[11] -
c3*(-A + Q1*y[9] + Q2*y[10] + Q3*y[11]))/
(-c3*y[10] + c2*y[11])) +
((-c3*y[9] + c1*y[11])*(-(-d3*p3*y[10] + (d3*p2 - d2*p4)*y[11])*
((-C - E1 + c1*Q1 + c2*Q2 + c3*Q3)*y[11] -
c3*(-A + Q1*y[9] + Q2*y[10] + Q3*y[11])) +
(-c3*y[10] + c2*y[11])*
((-p4*(-D + J1 + d1*Q1 + d2*Q2 + d3*Q4) +
d3*(p1*Q1 + p2*Q2 + p3*Q3 + p4*Q4))*y[11] -
d3*p3*(-A + Q1*y[9] + Q2*y[10] + Q3*y[11])))/
((-c3*y[10] + c2*y[11])*((-c3*y[10] + c2*y[11])*(-d3*p3*y[9] +
(d3*p1 - d1*p4)*y[11]) -
(-c3*y[9] + c1*y[11])*(-d3*p3*y[10] + (d3*p2 - d2*p4)*y[11])));
}
else if (idx == 7){
return -((-A*c2 + c2*Q1*y[9] + C*y[10] + E1*y[10] -
c1*Q1*y[10] -c3*Q3*y[10] + c2*Q3*y[11])/
(-c3*y[10] + c2*y[11])) +
((c2*y[9] -c1*y[10])*(-(-d3*p3*y[10] + (d3*p2 - d2*p4)*y[11])*
((-C - E1 + c1*Q1 + c2*Q2 + c3*Q3)*y[11] -
c3*(-A + Q1*y[9] + Q2*y[10] + Q3*y[11])) + (-c3*y[10] +c2*y[11])*
((-p4*(-D + J1 + d1*Q1 + d2*Q2 + d3*Q4) +
d3*(p1*Q1 + p2*Q2 + p3*Q3 + p4*Q4))*y[11] -
d3*p3*(-A + Q1*y[9] + Q2*y[10] + Q3*y[11])))/
```

```
((-c3*y[10] + c2*y[11])*((-c3*y[10] + c2*y[11])*
(-d3*p3*y[9] + (d3*p1 - d1*p4)*y[11]) -
(-c3*y[9] + c1*y[11])*(-d3*p3*y[10] + (d3*p2 - d2*p4)*y[11])));
}
else if (idx == 8){
return -((-D + J1 + d1*Q1 + d2*Q2 + d3*Q4)/d3) +
(d2*((-C - E1 + c1*Q1 + c2*Q2 + c3*Q3)*y[11] -
c3*(-A + Q1*y[9] + Q2*y[10] + Q3*y[11])))/
(d3*(-c3*y[10] + c2*y[11])) +
((d1/d3 - (d2*(-c3*y[9] + c1*y[11]))/(d3*(-c3*y[10] + c2*y[11])))*
(-(-d3*p3*y[10] + (d3*p2 - d2*p4)*y[11])*
((-C -E1 + c1*Q1 + c2*Q2 + c3*Q3)*y[11] -
c3*(- A + Q1*y[9] + Q2*y[10] + Q3*y[11])) + (-c3*y[10] + c2*y[11])*
((-p4*(-D + J1 + d1*Q1 + d2*Q2 + d3*Q4) +
d3*(p1*Q1 + p2*Q2 + p3*Q3 + p4*Q4))*y[11] -
d3*p3*(-A + Q1*y[9] + Q2*y[10] + Q3*y[11])))/
((-c3*y[10] + c2*y[11])*(-d3*p3*y[9] + (d3*p1 - d1*p4)*y[11])-
(-c3*y[9] + c1*y[11])*(-d3*p3*y[10] + (d3*p2 - d2*p4)*y[11]));
}
else if (idx == 9) {
return /*-((beta*(-D + J1 + d1*Q1 + d2*Q2 + d3*Q4)*
z*(z - 2*y[1])*y[5])/(d3*p*q)) +
(2*alpha*beta*z*pow(sin(y[2]),2)*y[1]*y[5]*
(-A + Q1*y[9] +Q2*y[10] + Q3*y[11]))/(p*q*y[11]) -
(1/p)*(-((2*alpha*beta*pow(sin(y[2]),2)*(z*(-1 + y[1])*y[1]+
q*(z - 3*pow(y[1],2)))*
```

```
pow(y[5],2)*y[7])/pow(q,2)) -
(2*alpha*beta*(z + 2*pow(alpha,2)*pow(sin(y[2]),2))*
sin(2*y[2])*y[1]*y[5]*y[6]*y[7])/q -
2*alpha*beta*pow(sin(y[2]),2)*pow(y[1],2)*pow(y[6],2)*y[7] -
(1/(q*pow(z,2)))*2*alpha*beta*pow(sin(y[2]),4)*y[1]*(z*(z - 2*y[1])*
y[1]*(pow(y[1],2)+pow(alpha,2))+pow(alpha,2)*pow(sin(y[2]),2)*
(q*z - 2*pow(alpha,2)*pow(sin(y[2]),2)*pow(y[1],2) +
4*pow(y[1],3)))*pow(y[7],3) -(beta*(3*psi*q + pow(alpha,2)*z*pow(sin(y[2]),2)*
(1 - y[1]))*pow(y[5],2)*y[8])/pow(q,2) -
(pow(alpha,2)*beta*sin(2*y[2])*(z - 4*y[1])*y[5]*y[6]*y[8])/q -
beta*(z - 2*y[1])*y[1]*pow(y[6],2)*y[8] -
(beta*pow(sin(y[2]),2)*(-pow(alpha,2)*psi*
pow(sin(y[2]),2)*(z - 6*y[1]) +
pow(z,2)*(z - 2*y[1])*y[1])*pow(y[7],2)*y[8])/
pow(z,2) - (2*alpha*beta*psi*pow(sin(y[2]),2)*
(z - 3*y[1])*y[7]*pow(y[8],2))/pow(z,2) +
(beta*psi*(z - 2*y[1])*pow(y[8],3))/pow(z,2) -
(alpha*pow(sin(y[2]),2)*
(pow(alpha,2) - pow(y[1],2))*y[5]*y[7]*y[9])/q +
(pow(alpha,3)*pow(sin(y[2]),2)*sin(2*y[2])*y[1]*y[6]*y[7]*y[9])/z -
(pow(alpha,2)*pow(sin(y[2]),2)*(-1 + y[1])*y[5]*y[8]*y[9])/q +
(0.5*pow(alpha,2)*sin(2*y[2])*(z - 2*y[1])*y[6]*y[8]*y[9])/z -
(alpha*sin(2*y[2])*y[1]*y[5]*y[7]*y[10])/q -
(2*pow(sin(y[2]),2)*pow(y[1],2)*y[6]*y[7]*y[10])/z -
(0.5*pow(alpha,2)*sin(2*y[2])*(z - 4*y[1])*y[5]*y[8]*y[10])/(q*z) -
((z - 2*y[1])*y[1]*y[6]*y[8]*y[10])/z -
```

```
(alpha*psi*pow(y[5],2)*y[11])/pow(q,2) +
(2*alpha*pow(tan(y[2]),-1)*y[1]*y[5]*y[6]*y[11])/q -
(2*alpha*pow(sin(y[2]),2)*y[1]*
(-pow(alpha,2)*psi*pow(sin(y[2]),2) +
z*(z - 2*y[1])*y[1])*pow(y[7],2)*y[11])/(q*pow(z,2)) -
((-pow(alpha,2)*psi*pow(sin(y[2]),2)*(z - 4*y[1]) +
z*pow((z - 2*y[1]),2)*y[1])*y[7]*y[8]*y[11])/(q*pow(z,2)) -
(alpha*psi*(z - 2*y[1])*pow(y[8],2)*y[11])/(q*pow(z,2))) +
(1/(-c3*y[10] + c2*y[11]))*
((beta*d2*z*(z - 2*y[1])*y[5])/(d3*p*q) -
(2*alpha*beta*z*pow(sin(y[2]),2)*y[1]*y[5]*y[10])/(p*q*y[11]))*
((-C - E1 + c1*Q1 + c2*Q2 + c3*Q3)*y[11] -
c3*(-A + Q1*y[9] +Q2*y[10] + Q3*y[11])) +
(((beta*d1*z*(z - 2*y[1])*y[5])/(d3*p*q) +
(-((2*alpha*beta*z*pow(sin(y[2]),2)*y[1]*y[7])/q) +
(beta*z*(z - 2*y[1])*y[8])/q)/p -
(2*alpha*beta*z*pow(sin(y[2]),2)*y[1]*y[5]*y[9])/(p*q*y[11]) -
(((beta*d2*z*(z - 2*y[1])*y[5])/(d3*p*q) -
(2*alpha*beta*z*pow(sin(y[2]),2)*y[1]*y[5]*y[10])/(p*q*y[11]))*
(-c3*y[9] + c1*y[11]))/(-c3*y[10] + c2*y[11]))*
(-(-d3*p3*y[10] + (d3*p2 - d2*p4)*y[11])*
((-C - E1 + c1*Q1 + c2*Q2 + c3*Q3)*y[11] -
c3*(-A + Q1*y[9] + Q2*y[10] + Q3*y[11])) +
(-c3*y[10] + c2*y[11])*
((-p4*(-D + J1 + d1*Q1 + d2*Q2 + d3*Q4) +
d3*(p1*Q1 + p2*Q2 + p3*Q3 + p4*Q4))*y[11] -
```

```
d3*p3*(-A + Q1*y[9] +Q2*y[10] +
Q3*y[11])))/((-c3*y[10] + c2*y[11])*(-d3*p3*y[9] + (d3*p1 - d1*p4)*y[11]) -
(-c3*y[9] + c1*y[11])*(-d3*p3*y[10] + (d3*p2 - d2*p4)*y[11]))*/0.;
}
else if (idx == 10) {
return -((beta*(-D + J1 + d1*Q1 + d2*Q2 +
d3*Q4)*z*(z - 2*y[1])*y[6])/(d3*p)) -
(2*alpha*beta*z*pow(sin(y[2]),2)*y[1]*y[6]*
(-A + Q1*y[9] + Q2*y[10] + Q3*y[11]))/(p*y[11]) -
(1/p)*((2*pow(alpha,3)*beta*cos(y[2])*pow(sin(y[2]),3)*
y[1]*pow(y[5],2)*y[7])/q +
2*alpha*beta*eta*pow(sin(y[2]),2)*y[5]*y[6]*y[7] -
alpha*beta*(2*z + 3*pow(alpha,2)*pow(sin(y[2]),2))*
sin(2*y[2])*y[1]*pow(y[6],2)*y[7] -
(2*alpha*beta*cos(y[2])*pow(sin(y[2]),3)*y[1]*
((pow(y[1],2)+pow(alpha,2))*pow(z,2) +
4*pow(alpha,2)*z*pow(sin(y[2]),2)*y[1] + 2*pow(alpha,4)*y[1]*
pow(sin(y[2]),4))*pow(y[7],3))/pow(z,2) -
(0.5*pow(alpha,2)*beta*sin(2*y[2])*
(-z + 2*y[1])*pow(y[5],2)*y[8])/q -
2*beta*(4*pow(y[1],2) - z*(1 + y[1]))*y[5]*y[6]*y[8] -
pow(alpha,2)*beta*cos(y[2])*sin(y[2])*(z - 6*y[1])*pow(y[6],2)*y[8] -
(0.5*beta*sin(2*y[2])*(q*pow(z,3) + 2*pow(alpha,2)*
pow(sin(y[2]),2)*y[1]*(q*z - 6*(pow(y[1],2)+
pow(alpha,2))*y[1]))*pow(y[7],2)*y[8])/pow(z,2) -
(2*alpha*beta*sin(2*y[2])*y[1]*(-(pow(y[1],2)+pow(alpha,2))*(z - 2*y[1]) +
```

```
pow(alpha,2)*pow(sin(y[2]),2)*y[1])*y[7]*pow(y[8],2))/pow(z,2) -
(pow(alpha,2)*beta*sin(2*y[2])*(z - 2*y[1])*y[1]*pow(y[8],3))/pow(z,2) +
(2*pow(alpha,3)*cos(y[2])*pow(sin(y[2]),3)*y[1]*y[5]*y[7]*y[9])/z -
(alpha*q*pow(sin(y[2]),2)*(z - 4*pow(y[1],2))*y[6]*y[7]*y[9])/z -
(0.5*pow(alpha,2)*sin(2*y[2])*(-z + 2*y[1])*y[5]*y[8]*y[9])/z -
(q*(4*pow(y[1],2) - z*(1 + y[1]))*y[6]*y[8]*y[9])/z -
(2*alpha*pow(sin(y[2]),2)*
pow(y[1],2)*y[5]*y[7]*y[10])/z -
alpha*sin(2*y[2])*y[1]*y[6]*y[7]*y[10] -
((z - 2*y[1])*y[1]*y[5]*y[8]*y[10])/z +
0.5*pow(alpha,2)*sin(2*y[2])*y[6]*y[8]*y[10] -
(alpha*(-z + 2*pow(y[1],2))*y[5]*y[6]*y[11])/q +
2*alpha*pow(tan(y[2]),-1)*y[1]*pow(y[6],2)*y[11] -
(alpha*sin(2*y[2])*y[1]*(z + 2*pow(alpha,2)*pow(sin(y[2]),2)*y[1])*
pow(y[7],2)*y[11])/pow(z,2) -
(pow(tan(y[2]),-1)*(pow(z,3) + 2*z*(-z + pow(alpha,2)*pow(sin(y[2]),2))*y[1]-
8*pow(alpha,2)*pow(sin(y[2]),2)*pow(y[1],2))*y[7]*y[8]*y[11])/pow(z,2) -
(2*alpha*pow(tan(y[2]),-1)*y[1]*(-z + 2*y[1])*
pow(y[8],2)*y[11])/pow(z,2)) +
(1/(-c3*y[10] + c2*y[11]))*((beta*d2*z*(z - 2*y[1])*y[6])/(d3*p) +
(2*alpha*beta*z*pow(sin(y[2]),2)*y[1]*y[7] + beta*z*(z - 2*y[1])*y[8])/p +
(2*alpha*beta*z*pow(sin(y[2]),2)*y[1]*y[6]*y[10])/(p*y[11]))*
((-C - E1 + c1*Q1 + c2*Q2 + c3*Q3)*y[11] -
c3*(-A + Q1*y[9] +Q2*y[10] + Q3*y[11])) +
(((beta*d1*z*(z - 2*y[1])*y[6])/(d3*p) +
(2*alpha*beta*z*pow(sin(y[2]),2)*y[1]*y[6]*y[9])/(p*y[11]) -
```

```
(1/(-c3*y[10] + c2*y[11]))*((beta*d2*z*(z - 2*y[1])*y[6])/(d3*p) +
(2*alpha*beta*z*pow(sin(y[2]),2)*y[1]*y[7] + beta*z*(z - 2*y[1])*y[8])/p +
(2*alpha*beta*z*pow(sin(y[2]),2)*y[1]*y[6]*y[10])/(p*y[11]))*
(-c3*y[9] + c1*y[11]))*(-(-d3*p3*y[10] + (d3*p2 - d2*p4)*y[11])*
((-C - E1 + c1*Q1 + c2*Q2 + c3*Q3)*y[11] -
c3*(- A + Q1*y[9] +Q2*y[10] +
Q3*y[11])) + (- c3*y[10] + c2*y[11])*((-p4*(-D + J1 + d1*Q1 + d2*Q2 + d3*Q4)
+
d3*(p1*Q1 + p2*Q2 + p3*Q3 + p4*Q4))*y[11] - d3*p3*(-A + Q1*y[9] +Q2*y[10]
+
Q3*y[11])))/((-c3*y[10] + c2*y[11])*(-d3*p3*y[9] +
(d3*p1 - d1*p4)*y[11]) - (-c3 *y[9] + c1*y[11]) *
(-d3*p3*y[10] + (d3*p2 - d2*p4)*y[11]));
}
else if (idx == 11) {
return /*-((beta*q*(-D + J1 + d1*Q1 + d2*Q2 + d3*Q4)*
z*pow(sin(y[2]),2)*y[7])/(d3*p)) +
(beta*q*z*pow(sin(y[2]),2)*y[8]*
(- A + Q1*y[9] +Q2*y[10] + Q3*y[11]))/(p*y[11]) -
(1/p)*((2*alpha*beta*((pow(y[1],2)+pow(alpha,2))*psi +
2*z*pow(y[1],2))*pow(sin(y[2]),4)*y[5]*pow(y[7],2))/z -
(4*pow(alpha,3)*beta*q*cos(y[2])*pow(sin(y[2]),5)*
y[1]*y[6]*pow(y[7],2))/z +
(2*beta*pow(sin(y[2]),2)*(-psi*((pow(y[1],2)+pow(alpha,2)) +
pow(alpha,2)*pow(sin(y[2]),2)) +
z*(z - 2*y[1])*y[1])*y[5]*y[7]*y[8])/z +
```

```
beta*q*z*sin(2*y[2])*y[6]*y[7]*y[8] +
(2*alpha*beta*psi*pow(sin(y[2]),2)*y[5]*pow(y[8],2))/z -
(2*alpha*beta*q*sin(2*y[2])*y[1]*y[6]*pow(y[8],2))/z +
(alpha*q*pow(sin(y[2]),4)*(pow(alpha,2)*psi + pow(y[1],2)*
(z + 2*pow(y[1],2)))*pow(y[7],2)*y[9])/pow(z,2) -
(q*pow(sin(y[2]),2)*(psi*((pow(y[1],2)+pow(alpha,2)) +
pow(alpha,2)*pow(sin(y[2]),2)) +
z *y[1]*(-z + 2*y[1]))*y[7]*y[8]*y[9])/pow(z,2) +
(alpha*psi*q*pow(sin(y[2]),2)*pow(y[8],2)*y[9])/pow(z,2) -
(2*pow(alpha,3)*q*cos(y[2])*pow(sin(y[2]),5)*y[1]*
pow(y[7],2)*y[10])/pow(z,2) +
(0.5*q*sin(2*y[2])*(pow(z,2) + 4*pow(alpha,2)*pow(sin(y[2]),2)*y[1])*
y[7]*y[8]*y[10])/pow(z,4) -
(alpha*q*sin(2*y[2])*y[1]*pow(y[8],2)*y[10])/pow(z,2) -
(alpha*pow(sin(y[2]),2)*(-2*pow(alpha,2)*pow(sin(y[2]),2)*
pow(y[1],2) - 4*pow(y[1],3) +
(pow(y[1],2)+pow(alpha,2))*(-z + 4*pow(y[1],2)))*
y[5]*y[7]*y[11])/(q*z) +
(2*pow(alpha,3)*cos(y[2])*pow(sin(y[2]),3)*y[1]*y[6]*y[7]*y[11])/z -
((pow((z - 2*y[1]),2)*y[1] + pow(alpha,2)*sin(y[2])*
(z - 2*pow(y[1],2)))*y[5]*y[8]*y[11])/(q*z) -
(pow(tan(y[2]),-1)*(z*(z - 2*y[1]) + 2*pow(alpha,2)*
pow(sin(y[2]),2)*y[1])*y[6]*y[8]*y[11])/z) +
(beta*q*z*pow(sin(y[2]),2)*(-d3*y[8]*y[10] + d2* y[7]* y[11])*
((-C - E1 + c1*Q1 + c2*Q2 + c3*Q3)*y[11] -
c3*(-A + Q1*y[9] +Q2*y[10] + Q3*y[11])))/
```

```
(d3*p*y[11]*(-c3*y[10] + c2*y[11])) +
(((beta*q*z*pow(sin(y[2]),2)*
(-d3*y[8]*y[9] + d1*y[7]*y[11]))/(d3*p*y[11]) -
(beta*q*z*pow(sin(y[2]),2)*(-c3*y[9] + c1*y[11])*
(-d3*y[8]*y[10] + d2*y[7]*y[11]))/
(d3*p*y[11]*(-c3*y[10] + c2*y[11])))*
(-(-d3*p3*y[10] + (d3*p2 - d2*p4)* y[11])*
((-C - E1 + c1*Q1 + c2*Q2 + c3*Q3)*y[11] -
c3*(-A + Q1*y[9] + Q2*y[10] + Q3*y[11])) +
(-c3*y[10] + c2*y[11])*
((-p4*(-D + J1 + d1*Q1 + d2*Q2 + d3*Q4) +
d3*(p1*Q1 + p2*Q2 + p3*Q3 + p4*Q4))*y[11] -
d3*p3*(-A + Q1*y[9] + Q2*y[10] + Q3*y[11])))/
((-c3*y[10] + c2*y[11])*(-d3*p3*y[9] + (d3*p1 - d1*p4)*y[11]) -
(-c3*y[9] + c1*y[11])*(-d3*p3*y[10] + (d3*p2 - d2*p4)*y[11]))*/0.;
}
```

Bibliography

[1] Tanaka T, Mino Y, Sasaki M, and Shibata, M. *Gravitational waves from a spinning particle in circular orbits around a rotating black hole* Phys. Rev. D **54**, 3762 (1996)

[2] Faruque, S. B. *Gravitomagnetic clock effect in the orbit of a spinning particle orbiting the Kerr black hole* Physics Letters A **327**, 95-97 (2004)

[3] Mino, Y., Shibata M., and Tanaka, T. *Gravitational waves induced by a spinning particle falling into a rotating black hole* Phys. Rev D **53**, 622 (1996)

[4] Wald, R. *Gravitational Spin Interaction* Phys. Rev. D **6**, 406 (1972)

[5] Dixon, W. G. *Dynamics of extended bodies in General Relativity III. Equations of motion,* Proc. R. Soc. London **A** 319, 509 (1974)

[6] Carter, B. *Global Structure of the Kerr Family of Gravitatonal Fields* Phys. Rev. **174**, 1559 (1968)

[7] Papapetrou, A. *Spinning test - particles in general relativity I* Proc. R. Soc. London A **209**, 248 (1951)

[8] Mathisson, M. *Republication of: New Mechanics of Material Systems* Gen. Rel Grav. **42**, 1011 (2010)

[9] Ihan, I. *Dynamics of Extended Objects in General Relativity* arXiv:0911.3645v1 [gr-qc] 18 Nov 2009

[10] Dixon, W. G. *Dynamics of extended bodies in general relativity. I Momentum and angular momentum* Proc. Roy. Soc of London A **314**, 499 (1970)

[11] Mashhoon, B., and Singh, D. *Dynamics of extended spinning masses in a gravitational field*. Phys. Rev. D **74**, 124006 (2006)

[12] Kyrian, K, and Semerák, O. *Spinning test particles in a Kerr field - II* Mon. Not. R. Astron. Soc. **382**, 1922 (2007)

[13] Semerák, O. *Spinning test particles in a Kerr field - I* Mon. Not. R. Astron. Soc. **308**, 863-875 (1999)

[14] Faruque, S. B. *Gravitomagnetic clock effect in the orbit of a spinning particle orbiting the Kerr black hole* Phys. Lett. A **327,** 95-97 (2004)

[15] Plyatsko, R.M., Stefanyshyn, O.B., and Fenyk, M.T. *Mathisson-Papapetrou-Dixon equations in the Schwarzschild and Kerr backgrounds* Class. Quantum Grav. **28**, 195025 (2011)

[16] Bardeen, J., Press W., and Teukolsky A. *Rotating Black Holes: Locally non-rotating frames, energy extraction, and scalar synchrotron radiation* Astrophy. Journal, **178**, 347 (1972)

[17] Dadhich, N., and Kale, P.P. *Equatorial circular geodesics in the Kerr-Newman* J. Math. Phys. 18, 1727 (1977). Soc. A **314**, 499 (1970)

[18] Kheng L, Perng S, and Sze T *Massive particle orbits around Kerr Black Hole* (2007). (Unpublished)

[19] Teo, E. *Spherical Photon Orbits around a Kerr Black Hole* Gen. Relat. and Gravit. Vol. **35**, No. 11, 1909 (2003)

[20] Wilkins, D. *Bound Geodesics in the Kerr Metric* Phys. Rev. D **5**, 814 (1972)

[21] Tsoubelis, D., Economou, A., and Stoghianidis, E. *The geodetic effect along polar orbits in the Kerr spacetime* Phys. Lett. A, **118**, 113 (1986)

[22] Tsoubelis, D., Economou, A., and Stoghianidis, E. *Local and global gravitomagnetic effects in Kerr spacetime* Phys. Rev. D **36**, 1045 (1987)

[23] Stoghianidis, E., and Tsoubelis, D. *Polar Orbits in the Kerr Space-Time* Gen. Relat. and Gravit. vol **19**, No. 12 (1987)

[24] Tod K.P., and De Felice, F. *Spinning test particles in the Field of a Black Hole* Il Nuovo Cimento B **34**, 365 (1976)

[25] Abramowicz, M., and Calvani, M. *Spinning particles orbiting the Kerr black hole* Mon. Not. R. astr. Soc. **189**, 621-626 (1979)

[26] Mashhoon, B., Gronwald, F., and Lichtenegger, H.I. *Gravitomagnetism and the Clock Effect* Lect. Notes Phys. **562**, 83 (2001)

[27] Everitt, C. W. *et al. Gravity Probe B Data Analysis Space* Sci Rev **148**, 53 (2009)

[28] Everitt, C. W. *et al. Gravity Probe B: Final Results of a Space Experiment to Test General Relativity* Phys. Rev Lett **106**, 221101 (2011)

[29] Capderou, Michel *Satellites, Orbits and Missions* Springer, Paris (2005)

[30] Tejeiro, J.M. *Fundamentos de Relatividad General* Apuntes de Clase. Bogotá, Universidad Nacional de Colombia (2004)

[31] Boyer, R., and Lindquist, R. *Maximal Analytic Extension of the Kerr Metric* Journal of mathematical physics vol **8**, number 2 (1967)

[32] Hagihara, Y. *Celestial Mechanics*, MIT Press, Cambridge, Mass., 1970

[33] Ruggiero, M.L. and Tartaglia, A. *Gravitomagnetic effects* Nuovo Cim. B **117**, 743 (2002)

[34] Iorio, I., and Corda, C. *Gravitomagnetism and gravitational waves* The Open Astronomy Journal **4**, 84 (2011)

[35] Hobson, M., Efstathiou, G., and Lasenby, A. *General Relativity. An Introduction for Physicists* Cambridge: University Press Cambridge (2006)

[36] Beiglböck, W. *The Center of Mass in Einstein´s Theory of Gravitation.* Commun. math. Phys. **5**, 106-130 (1967)

[37] Almonacid, W. A. *Problema de los dos cuerpos extendidos en Relatividad General bajo la Aproximación Post-newtoniana* Tesis de maestría en Astronomía. Universidad Nacional de Colombia, Bogotá, (2013)

[38] Kunst, Daniela *General relativistic dynamics of spinning particles* Dissertation. Universität Bremen, (2015)

[39] Corinaldesi, E., and Papapetrou, A. *Spinning Test Particles in General Relativity II* Proc. Roy. soc. Lond. A **209**, 259 (1951)

[40] Karpov, O. B. *The Papapetrou equations and supplementary conditions.* arXiv:gr-qc/0406002v2 2 Jun 2004

[41] Pirani, F.A. *On the physical significance of the Riemann tensor* Acta Phys. Pol. **15**, 389 (1956)

[42] Costa F., Herdeiro C., Natario, J., and Zilhao M. *Mathisson´s helical motions for a spinning particle - are they unphysical?* arXiv:1109.1019v1

[43] Dixon, W. G. in *Isolated Gravitating Systems in General Relativity*, edited by J. Ehlers (North-Holland, Amsterdam, 1979), pp. 156-219

[44] Mashhoon, B. *Gravitational couplings of intrinsic spin* Class. Quantum Grav. **17**, 2399-2409 (2000)

[45] Costa, F., Natário, J., and Zilhao, M. *Spacetime dynamics of spinning particles - exact gravito-electromagnetic analogies* Phys. Rev. D **93**, 104006 (2016)

[46] Costa, F., Natário, J. *Center of mass, spin supplementary conditions, and the momentum of spinning particles.* Fundamental Theories of Physics **179**, 215 (2015)

[47] Dixon, W. in *Isolated Gravitating Systems in General Relativity*, edited by J. Ehlers (North-Holland, Amsterdam, 1979), pp. 156-219

[48] Iorio, L. *General relativistic spin-orbit and spin-spin effects on the motion of rotating particles in an external gravitational field* Gen Relat Gravit **44**, 719 (2012)

[49] Ferrari, V., and Gualtieri, L. *General Relativity: Chapter* **20** Sapienza Universita di Roma

[50] Chandrasekhar, S. *The mathematical Theory of Black Holes* Oxford University Press, 1983

[51] Susuki, S. and Maeda, K. *Innermost stable circular orbit of a spinning particle in Kerr spacetime* Physical Review D **58**, 023005 (1998)

[52] Levin, J., and Perez-Giz, G. *A Periodic Table for Black Hole orbits* Phys. Rev. D **77**, 103005 (2008)

[53] Mashhoon, B., and Singh, D. *Dynamics of extended spinning masses in a gravitational field* Phys. Rev D **74**, 124006 (2006)

[54] Chicone, C., Mashhoon, B., Punsly, B.: Relativistic motion of spinning particles in a gravitational field. Phys. Letters A **343**, 1 (2005

[55] Boccaletti & G. Pucacco *Theory of Orbits*, Springer-Verlag, Berlin 2001

[56] Plyastsko, R. and Fenyk, M. *Spinning particle in Schwarzschild´s field: circular and other highly relativistic orbits* Phys. Rev. D **85**, 104023 (2012)

[57] Mashhoon, B. *Gravitoelectromagnetism* Proc. Spanish Relativity Meeting (World Scientific, 2001)

[58] Plyatsko, R., and Fenyk, M. *Highly relativistic circular orbits of spinning particle in the Kerr field* Physical Review

[59] Plyatsko, R., Stefanyshyn, O., and Fenyk, M. *Highly relativistic spininning particle starting near* $r_{ph}^{(-)}$ *in a Kerr field* Physical Review D **82**, 044015 (2010)

[60] http://demonstrations.wolfram.com/3DKerrBlackHoleOrbits/**??** nn

[61] Costa F., Natário J., and Zilhao, M. *Spacetime dynamics of spinning particles - exact gravito-electromagnetic analogies* (2012)

[62] Costa F., and Herdeiro, C. *A gravito-electromagnetic analogy based on tidal tensors* Phys. Rev. D **78**, 024021 (2008)

[63] Bosi, F., Cella, G. and *et al. Measuring gravitomagnetics effects by a multi-ring-laser gyroscope* Phys. Rev. D **84**, 122002 (2011)

[64] Franklin, J, and Baker, P. T. *Linearized Kerr and spinning massive bodies: An electrodynamics analogy* Am. J. Phys. **75**, 336 (2007)

[65] Thirring, H. *On the formal analogy between the basic electromagnetic equations and Einstein´s gravity equations in first approximation.* Gen. Relativ. Gravit. **44**, 3225 (2012)

[66] Costa, F., Herdeiro, C. *A gravito-electromagnetic analogy based on tidal tensors.* Phys. Rev. D **78**, 024021 (2008)

[67] Cohen, J., Mashhoon, B. *Standard clocks, interferometry, and gravitomagnetism.* Phys. Letters A **181**, 353 (1993)

[68] Tulczyjew, W. Acta Phys. Pol. **18**, 393 (1959)

[69] Tartaglia, A. *Geometric Treatment of the Gravitomagnetic Clock Effect* Gen. Rel. Grav. **32**, 1745 (2000)

[70] Tartaglia, A. *Gravitomagnetism, clocks and geometry* Eur. J. Phys. 22, 105-111 (2001)

[71] Cahill, R. *The Michelson and Morley 1887 Experiment and the Discovery of Absolute Motion* Progr. Phys. **3,** 25 (2005)

[72] Crossley, D. *The Michelson-Morley experiment in an accelerated reference frame* Physics Essays **24**, 435 (2011)

[73] Tartaglia, A., and Ruggiero, M. *Angular momentum effects in Michelson-Morley type experiments* Gen. Rel. Grav. **34**, 1371 (2002)

[74] Plyatsko, R., and Fenyk, M. *Highly relativistic spinining particle in the Schwarzschild field: Circular and other orbits* Physical Review D **85**, 104023 (2012)

[75] Press, W., Teukolsky, S., Vetterling, W., and Flannery, B. *Numerical Recipes in C*. Cambridge University Press, New York (1997)

[76] Goldstein, H. *Mecánica clásica*. Barcelona: Editorial Reverté, S.A., 1987

[77] Costa, F., Herdeiro, C., Natário, J., and Zilhao, M. *Mathisson´s helical motions demystified*. AIP Conference Proceedings **1458**, 367 (2012)

[78] Gralla, S., Harte, A., and Wald, R. *Bobbing and Kicks in Electromagnetism and Gravity*. Phys. Rev. D **81,** (2010)

[79] Jackson, J. *Classical electrodynamics*. John Wiley & Sons, Inc., New York (1962)

[80] Mashhoon, B. *On the spin-rotation-gravity coupling* Gen. Rel. Grav. **31**, 681 (1999)

[81] Wen-Biao H., Shu-Cheng Y. *Exotic orbits due to spin-spin coupling around Kerr black holes*. Int. J. of M. Phy. D **26**, 1750179 (2017)

[82] Bini, D., Geralico, A., and Jantzen, R. *Kerr metric, static Observers and Fermi coordinate* Class. Quantum Grav. **22**, 4729 (2005)